Ago2-dependent processing allows miR-451 to evade the global microRNA turnover elicited during erythropoiesis

Dmitry A. Kretov[1], Isha Walawalkar[1], Alexandra Mora-Martin[1], Andrew Shafik[1,3], Simon Moxon[2], Daniel Cifuentes[1,†,*]

[1]Department of Biochemistry, Boston University School of Medicine, Boston, MA

[2]School of Biological Sciences, University of East Anglia, Norwich, UK

[3]Present Address: Department of Human Genetics, Emory University School of Medicine, Atlanta, GA

[†]Lead contact: Daniel Cifuentes

*Correspondence: dcb@bu.edu

SUMMARY

MicroRNAs are sequentially processed by two RNAse III enzymes, Drosha and Dicer. miR-451 is the only known miRNA whose processing bypasses Dicer and instead relies on the slicer activity of Argonaute-2 (Ago2). MiR-451 is highly conserved in vertebrates and regulates erythrocyte maturation, where it becomes the most abundant miRNA. However, the basis for the non-canonical biogenesis of miR-451 is unclear. Here we show that Ago2 is less efficient than Dicer in processing pre-miRNAs but this deficit is overcome when miR-144 represses Dicer in a negative feedback loop during erythropoiesis. Loss of miR-144 mediated Dicer repression in zebrafish embryos and human cells leads to increased canonical miRNA production and impaired miR-451 maturation. Over-expression of Ago2 rescues some of the defects of miR-451 processing. Thus, the evolution of Ago2-dependent processing allows miR-451 to circumvent the global repression of canonical miRNAs elicited in part by the miR-144 targeting of Dicer during erythropoiesis.

KEYWORDS

microRNA, erythropoiesis, miR-451, miR-144, Dicer, Ago2, zebrafish.

INTRODUCTION

Canonical microRNA (miRNA) processing involves the sequential cleavage of a primary miRNA transcript by two ribonuclease III enzymes, Drosha and Dicer (Treiber et al., 2019). The final product of this family of small non-coding RNAs is a ~22-nucleotide RNA that guides the members of the Argonaute family to mediate target mRNA translational repression, deadenylation and decay (Bartel, 2018).

Despite their stereotypic processing, several miRNAs have evolved to bypass the first committed step of Drosha processing. For instance, miRtrons are derived from intronic regions (Ruby et al., 2007, Okamura et al., 2007, Berezikov et al., 2007), and the corresponding splice sites define the ends of their precursor miRNAs (pre-miRNA). Pre-miRNAs can also arise from tRNA genes, where the 5' end is defined by RNAseZ cleavage and the 3' end corresponds to transcription termination by RNA polymerase III (Haussecker et al., 2010). Other Drosha-independent miRNAs are generated from certain small nucleolar RNA (snoRNAs) (Ender et al., 2008) or directly from the 5' end of Pol II-transcribed genes (Xie et al., 2013). Even herpes virus hijacks the Integrator complex to generate pre-miRNA hairpins that are subsequently processed by Dicer (Cazalla et al., 2011).

In contrast to these non-canonical miRNAs, miR-451, a vertebrate specific miRNA, is the only known example of a microRNA whose biogenesis is strictly independent of Dicer. The pre-miR-451 hairpin resulting from Drosha cleavage displays an unusually short stem that bypasses Dicer, and its maturation relies instead on the slicer activity of Argonaute-2 (Ago2), which cleaves the hairpin in the middle of its 3' arm (Yang et al., 2010, Cifuentes et al., 2010, Cheloufi et al., Nelson et al., 2007). This cleavage event is followed by 3'-to-5' trimming mediated by polyA-specific ribonuclease (PARN) to generate mature miR-451 (Yoda et al., 2013) (Figure 1A).

miR-451 is the most abundant miRNA in mature erythrocytes (Rasmussen et al., 2010, Pase et al., 2009, Zhan et al., 2007, Zhang et al., 2011, Nelson et al., 2007) and is refractory to the global down-regulation of canonical miRNAs that occurs during erythropoiesis (Zhang et al., 2011). The loss-of-function of miR-451 in zebrafish and mice leads to incomplete erythrocyte differentiation (Rasmussen et al., 2010, Pase et al., 2009) and increased susceptibility to oxidative stress (Patrick et al., 2010, Yu et al., 2010), whereas its gain-of-function is associated with polycythemia vera (Bruchova et al., 2007, Bruchova et al., 2008). While the unique biogenesis of miR-451 and its role in hematopoiesis have been extensively studied, it remains unclear why Ago2-dependent

processing of pre-miR-451 and its role in erythropoiesis is conserved across all vertebrates (Bartel, 2018, Yang et al., 2010, Yang and Lai, 2010).

Although miR-451 is encoded in the same primary transcript as Dicer-dependent miR-144 (Dore et al., 2008), we found a ~7.5-fold excess of miR-451 over miR-144 in zebrafish erythrocytes while our *in vivo* miRNA processing assays suggested that Dicer was more efficient than Ago2. We solve this paradox by uncovering a negative feedback loop involving miR-144 and Dicer, which leads to the demise of canonical miRNAs during erythropoiesis. Overall, our results show how the evolution of Ago2-dependent processing allows miR-451 to bypass the global microRNA turnover that occurs during vertebrate erythropoiesis and become the most abundant in erythrocytes.

RESULTS

Canonical miRNA biogenesis is more efficient than Ago2-dependent processing.

We hypothesized that the Ago2-depedent processing may have evolved to confer a competitive advantage to miR-451 over the biogenesis of canonical microRNAs. The miR-144/451 cluster provides a unique opportunity to test this hypothesis without the interference of transcriptional effects because both miRNAs are encoded in the same primary transcript but after the cleavage step catalyzed by Drosha, they are processed by Dicer and Ago2 respectively.

When we analyzed the accumulation of endogenous miR-451 and miR-144 by Northern blot, we observed 1.8-fold more miR-451 than miR-144 in 2-day-old zebrafish embryos and 7.5 fold increase in peripheral blood of adult fish (Figures S1A and S1B). In addition, small RNA sequencing data indicated that miR-451 becomes up to 25% of the total microRNA content of embryonic erythrocytes (Figure 1B). These results imply a difference in post-transcriptional regulation between miR-144 and miR-451 and are in line with the data available for mice (Zhang et al., 2011, Rasmussen et al., 2010), where this ratio grows to 100-fold and miR-451 becomes ~60% of total erythrocyte miRNA content (Figures S1E and S1F).

Next, we directly analyzed the pre-miRNA processing efficiency of Dicer and Ago2 enzymes in zebrafish embryos. In order to avoid sequence-dependent effects we tested the processing of wild-type zebrafish pre-miR-451 (pre-miR-451^{Ago2}) and pre-miR-451^{Dicer}, a reprogrammed version of the precursor that is processed by Dicer but produces the same mature miRNA as wild-type pre-miR-451 (Cifuentes et al., 2010). We introduced

bulges, changed loop size and switch mature arm to test other potential variables that can affect miRNA processing (Figure 1C). The Northern blot analysis revealed that pre-miR-451^{Ago2} was processed ~20-fold less efficiently on average than pre-miR-451^{Dicer} mimics (Figure 1D) in injected embryos. Accordingly, injection of pre-miR-451^{Dicer} into embryos resulted in greater repression (83%) of a yellow fluorescent protein miR-451 reporter with two imperfect target sites for miR-451 in its 3'UTR (EYFP-2xIPT-miR-451) compared to injection of wild-type pre-miR-451^{Ago2} (32%) (Figure 1E).

To gain more insight into the dynamics of Ago2-mediated pre-miRNA processing, we determined the percentage of precursor cleavage across different time points after injection into zebrafish embryos. We detected the initial accumulation of mature miR-451^{Dicer} 30 minutes after injection of the precursor, while mature miR-451^{Ago2} was not detected until 4 hours post-injection (hpi) (Figure 1F). In line with these results, we observed that while near 80% of pre-miR-451^{Dicer} is cleaved by 6 hpi, cleavage of pre-miR-451^{Ago2} barely reaches 20% (Figure 1G).

To discard that the efficiency of the Ago2-mediated cleavage step could be compensated by enhanced Drosha processing in erythrocytes, we analyzed the processing of pri-miR-451^{Ago2} and pri-miR-451^{Dicer} in the context of the miR-144/451 primary transcript. We observed a readily accumulation of pre-miR-451^{Ago2}, pre-miR-451^{Dicer} and pre-miR-144 at early time points (Figure S1C) and at a similar rate (Figure S1D), suggesting that Drosha-mediated cleavage step is not affected in pri-miR-451^{Ago2}. However, we observed again a severe impairment of the processing of pre-miR-451^{Ago2} to the mature product. Thus, the efficiency of the Ago2-dependent processing of miR-451 (or the lack thereof) cannot explain the high levels of miR-451 found in erythrocytes compared to canonical miRNAs.

miR-144 targets Dicer in a negative-feedback loop

To resolve the apparent paradox of the over-accumulation of endogenous miR-451 despite its poor processing when compared to Dicer-dependent miRNAs, we hypothesized that changes in the levels of Dicer during erythrocyte maturation may make the Ago2-dependent pathway more competitive. Analysis of recent mass spectrometry data of protein changes during human erythropoiesis (Gautier et al., 2016) revealed a steady decline in the protein levels of Dicer during erythrocyte differentiation, while the levels of Ago2 remained constant (Figure S2A). In addition, in blood isolated from 2-day-old zebrafish embryos we detected a 44% reduction in *dicer1* mRNA compared to its levels in the whole embryo, suggesting that Dicer may also be down-regulated in zebrafish

erythrocytes. We reasoned that the Dicer decline may be due to miR-451 targeting of the *dicer1* 3'UTR, as miR-451 is refractory to Dicer loss whereas canonical miRNAs are globally down-regulated (Zhang et al., 2011). However, we were unable to find any regions of the *dicer1* 3'UTR complementary to the miR-451 seed. We instead found 3 sites complementary to the miR-144-3p seed (Figure 2A). Predicted miR-144 sites were also found in the *dicer1* 3'UTRs of human (3 sites), mouse (1 site), rhesus (3 sites), chimp (2 sites), cow (1 site), dog (3 sites), rat (2 sites), opossum (6 sites), chicken (7 sites), and *Xenopus tropicalis* (1 site) (Agarwal et al., 2015) (Figure S2B). Some of these sites are in the same portion of the 3'UTR while others are specific to a given organisms. This pervasive conservation of miR-144 sites in *dicer1* 3'UTR across vertebrates suggests a potentially relevant physiological role for the miR-144-mediated repression of Dicer.

To validate Dicer as a target of miR-144, we performed reporter assays in zebrafish. A Nanoluciferase reporter coupled to the zebrafish *dicer1* 3'UTR (NLuc-*dicer1*$^{3'UTR\text{-}wt}$) was silenced only when co-injected with miR-144 duplex in zebrafish embryos (Figure 2B), whereas mutation of the predicted miR-144 target sites in the *dicer1* 3'UTR (NLuc-*dicer1*$^{3'UTR\text{-}mut}$) abrogated miR-144-mediated repression (Figure 2B). We obtained similar results using a yellow fluorescent protein with *dicer1* 3'UTR reporter (EYFP-*dicer1*$^{3'UTR}$) (Figure S3A). We also confirmed that miR-144 duplex represses ~20% NLuc signal when fused to human *dicer1* 3'UTR and co-transfected with miR-144 duplex into HEK293T cells (Figure S3B). Finally, we generated a zebrafish line where miR-144 is deleted and tested the levels of *dicer1* mRNA in peripheral blood by RT-QPCR. *Dicer1* mRNA was up-regulated 1.93-fold (SEM±0.22) in miR-144$^{\Delta/\Delta}$ compared to wild-type erythrocytes (Figure 2C). Thus, the *dicer1* 3'UTR confers sensitivity to miR-144 targeting *in vivo* and, as a result, Dicer expression is up-regulated specifically in erythrocytes of miR-144 mutants. Thus, these results suggest that miR-144 targets its own processing enzyme, Dicer, forming a negative feedback loop.

Next, we tested if de-repression of Dicer in miR-144 mutants has an impact in the processing of canonical miRNAs. We isolated peripheral blood from 2-day-old embryos and determined their small RNA populations by deep-sequencing. To take into account that miR-451 accumulates as mature miRNA but also as longer intermediate trimming species, for each miRNA we plotted the sum of all the pre-miRNA hairpin-matching reads. We observed a global increase in the abundance of miRNAs in the blood from miR-144$^{\Delta/\Delta}$ embryos compared to wild-type (Figure 2D), in concordance with the increase of Dicer expression in blood after loss of miR-144 (Figure 2C). We reasoned that the miR-144-mediated repression of Dicer is in part responsible, together with other potential

transcriptional factors and chromatin regulators, for the global down-regulation of canonical miRNA in erythrocytes.

Deletion of miR-144 or miR-451 impairs erythropoiesis.

To uncover the impact of the loss of miR-144 in erythropoiesis, we analyzed the hematopoietic phenotype of miR-144$^{\Delta/\Delta}$ embryos and compared it to miR-451$^{\Delta/\Delta}$ and wild-type embryos (Figure 3A). Northern blot analysis indicated that miR-144 and miR-451 were lost in the corresponding mutant line (Figure 3B). MiR-144$^{\Delta/\Delta}$ and miR-451$^{\Delta/\Delta}$ embryos were morphologically normal (Figure S4A) and survived to adulthood. However, transcriptome profiling of peripheral blood revealed stabilization of predicted miR-144 and miR-451 targets expressed in blood (Figure 3C). 2-day-old miR-451$^{\Delta/\Delta}$ embryos showed severe anemia under oxidative stress conditions induced by incubation with 0.003% phenylthiourea (Figures 3D, S4B) similar to miR-451 morphant embryos (Pase et al., 2009, Yu et al., 2010). Erythropoiesis was rescued by injection of miR-451 duplex at the one-cell stage (Figure S4C). In contrast, miR-144$^{\Delta/\Delta}$ embryos displayed levels of hemoglobinized cells similar to wild-type (Figures 3D and S4D). Quantitative analysis of blood smears from adult fish stained with May-Grünwald-Giemsa revealed that miR-144$^{\Delta/\Delta}$ as well as miR-451$^{\Delta/\Delta}$ erythrocytes have enlarged nuclei compared to wild-type fish (Figures 3E, 3F). In addition, miR-144$^{\Delta/\Delta}$ erythrocytes showed increased granular nuclear staining compared to wild-type cells (Figure 3G), indicative of impaired chromatin condensation. Since these phenotypes are observed in adult peripheral blood after it has left the hematopoietic tissue, these results suggest that erythrocyte maturation is impaired, rather than delayed, in miR-144$^{\Delta/\Delta}$. The fact that loss of Ago2 recapitulates both phenotypes highlights its central role as an essential factor for miRNA stability and the fact that is the main Argonaute paralogue expressed in blood (Cifuentes et al., 2010, Jee et al., 2018).

Deletion of miR-144 impairs miR-451 processing in *trans*.

Although miR-451 biogenesis bypasses Dicer, Northern blot analysis of 2-day-old miR-144$^{\Delta/\Delta}$ mutant embryos revealed that pre-miR-451 processing was affected (Figure 3B). Specifically, we observed a decrease of mature miR-451 product (23 nt), accompanied by increased levels of intermediate trimming products (24-29 nt) (Figure 3H, S3C and S4H), while the levels of pre-miR-451 remained largely unchanged. The fact that deletion of miR-144 does not affect the expression levels of the miR-451 primary transcript (Figure S4G), together with the accumulation of trimming intermediates, explains why we observe an increase in miR-451 hairpin-matching reads in Figure 2D.

Additionally, we observed that miR-144/451 expression peaks at 48 hpf and that the impaired trimming phenotype was ameliorated later in development (Figure S3C). We reasoned that at the peak of expression, the amount of miR-144/451 expression saturates the processing machinery, specifically at the trimming step, and this saturation was exacerbated in the miR-144$^{\Delta/\Delta}$ mutant likely due to the increase of canonical miRNA production.

PARN is the enzyme responsible for the trimming of the 3'-end of miR-451 (Yoda et al., 2013) and also of many canonical miRNAs (Shukla et al., 2019, Lee et al., 2019). Since loss of miR-144 did not alter PARN expression in blood (Figure S4E), we speculated that the increase of canonical miRNAs driven by the loss of miR-144 and concomitant stabilization of Dicer leads to a competition between miR-451 and canonical miRNAs for PARN-mediated trimming. This competition is resolved with time, once the erythrocytes mature.

The fact that the trimming intermediates but not the pre-miR-451 levels were affected in the miR-144$^{\Delta/\Delta}$ mutant suggested a role of miR-144 interfering with miR-451 processing in *trans,* once both miRNAs have been excised from the primary transcript by Drosha-mediated cleavage. Indeed, miR-451 processing from a primary transcript with the miR-144 deleted was similar to the processing of the wild-type locus (Figure S3D and S3E) and miR-144 duplex injection partially rescued the trimming defect in miR-144$^{\Delta/\Delta}$ mutant embryos (Figure 3I). The increase in miR-451 trimming intermediates is not accompanied by a change in the expression of miR-451 targets (Figure S4F), as these miRNA species are still competent to elicit miRNA-mediated repression (Yoda et al., 2013). In addition, other transcriptional and post-transcriptional mechanisms could be redundant with miR-144 to mediate the repression of Dicer and might buffer the effects of the loss of miR-144.

We also observed a reduction of miR-144 in miR-451$^{\Delta/\Delta}$ mutants (Figure 3B and S4I) and a consequent partial stabilization of miR-144 targets (Figure S4F). However, miR-451 deletion reduced the levels of miR-144 primary transcript embryos and injection of miR-451 duplex did not rescue miR-144 accumulation in miR-451$^{\Delta/\Delta}$ (Figure S4G and S4I), although miR-144 levels are normalized in adult blood (Figure S4J). We speculate that deletion of miR-451 may influence the biogenesis of miR-144 mainly in *cis*, by altering the stability of the mutant primary transcript.

To test if the action in *trans* of miR-144 over miR-451 is mediated through the targeting

of Dicer *in vivo*, we took advantage of Dicer mutant embryos (Wienholds et al., 2003) to genetically alter the levels of Dicer and interrogate miR-451 biogenesis. We extracted RNA from peripheral blood of adult miR-144$^{\Delta/\Delta}$ mutants (Figure 2C), and from Dicer$^{hu896/+}$ adult zebrafish, which express only one functional allele of Dicer. Northern blot analysis revealed an increased accumulation of the Dicer-dependent miRNA let-7 in miR-144$^{\Delta/\Delta}$ mutant compared to wild-type (Figure 3J), indicating that loss of miR-144$^{\Delta/\Delta}$ also upregulates canonical miRNA in adult fish during definitive erythropoiesis as we observed in embryos (Figure 2D). We did not detect in adults the reduction in mature miR-451 that we saw in miR-144$^{\Delta/\Delta}$ mutant embryos (Figure 3B, 3H and S3C), probably due to the fact that in the adult, the mature erythrocytes have been in circulation enough time to fully resolve miR-451 trimming. However, miR-451 accumulated in Dicer heterozygous fish, indicating that miR-451 levels are indeed linked to Dicer expression.

Altogether, these results provide ample evidence on how alteration of Dicer levels, in part through miR-144 activity, influences miR-451 processing and provide a unique example of how a miRNA can affect the processing of a clustered miRNA in *trans*.

Manipulation of the miR-144/Dicer negative feedback loop affects miR-451 biogenesis.

To determine the mechanism of miR-451 regulation by miR-144 and its conservation in vertebrates, specifically in mammals, we reconstructed the miR-144/Dicer negative feedback loop in mouse and human cell lines. First, we tested the impact of Dicer levels on miR-451 processing. We over-expressed the FLAG-tagged coding sequence of human Dicer in *dicer1* knockout mouse embryonic fibroblasts (Dicer KO MEFs) co-transfected with the plasmid encoding human miR-144/451 cluster (Figures 4A and 4B). Dicer over-expression had a significant impact on miRNA biogenesis, increasing miR-144 by 5.3-fold ($p=0.004$) and endogenous *let-7* by 12.3-fold ($p<0.0001$) but repressing miR-451 by 2-fold ($p=0.004$) (Figure 4C, 4D and 4E). Over-expression of a catalytically dead Dicer did not increase the impaired miR-144 or *let-7* expression and miR-451 biogenesis remained similar to control cells. We obtained similar results in HEK293T cells (Figure 4F, S5A and S5B), albeit with reduced effects on miR-451 processing probably due to pre-existing levels of mature canonical miRNAs (Figures S5A, S5B, S5C). In HEK293T cells, catalytically dead Dicer acted in a dominant negative manner and reduced canonical miRNA processing while enhancing miR-451 biogenesis (Figures 4F and S5A). These results demonstrate that high levels of canonical miRNAs negatively impact the processing of miR-451, suggesting there is competition between the two pathways.

To test if miR-144 affects miR-451 processing in *trans* through its targeting of Dicer, we transfected a plasmid encoding the human *dicer1* gene with its full-length wild-type 3'UTR that includes three miR-144 sites into HEK293T cells (Figure S2B). Over-expression of *dicer1*$^{+3'UTR}$ did not affect the processing of pre-miR-451 (Figure 5A, 5B). However, the transfection of the miR-144/451 cluster with the seed of miR-144 mutated caused the de-repression of *dicer1*$^{+3'UTR}$ and its stabilization at protein level by 1.37-fold (SEM±0.10, p=0.0029) compared to cells transfected with wild-type miR-144 (Figure 5C and 5D) and reduced pre-miR-451 processing (0.64-fold, p=0.0044) (Figure 5A and 5B). Since the seed mutation in miR-144 does not alter the overall predicted secondary structure of the cluster (Figure S6A) and therefore all potential *cis*-regulation of miR-451 processing remains intact, these results suggest that miR-144 enhances miR-451 biogenesis in *trans* by repressing Dicer and in turn, repressing global canonical miRNA processing.

To test whether the defect in miR-451 processing in miR-144$^{\Delta/\Delta}$ was caused by sequestration of pre-miR-451 by Dicer, we pulled down FLAG-tagged Dicer from zebrafish embryos co-injected with pre-miR-451^{Ago2} or pre-miR-451^{Dicer}. In these conditions, only pre-miR-451^{Dicer} and mature miR-451^{Dicer} were associated with Dicer (Figure S6B), indicating that the increased levels of Dicer in miR-144$^{\Delta/\Delta}$ do not titrate away the pre-miR-451 available for Ago2 processing by sequestering the pre-miR-451^{Ago2} precursor.

Both Ago2- and Dicer-dependent pathways compete for Ago2

Finally, we reasoned than an increase in canonical miRNAs would perturb miR-451 biogenesis due to their increased occupancy of Ago2. To test this hypothesis, we over-expressed Ago2 in HEK293T cells and Dicer KO MEFs and observed the rescue of the miR-451 processing defects induced by Dicer over-expression (Figures 5E, 5F, 5G, S6C). This observation confirms that Ago2 is the terminal acceptor of miRNAs that are produces from both pathways.

Ago2 over-expression also allowed the efficient processing of pre-miR-451 in zebrafish to the levels comparable to a Dicer-dependent hairpin mimic (Figure 5H). Over-expression of mouse Ago2 (*Mm*Ago2) enhanced pre-miR-451 processing to a greater extent than the zebrafish ortholog (*Dr*Ago2) (2.2-fold), consistent with the sub-optimal catalytic site in *Dr*Ago2 (Chen et al., 2017). These results also highlight how the slicing activity of Ago2 is a limiting factor for pre-miR-451 processing.

Altogether, these results demonstrate that the efficient processing of pre-miR-451 requires the repression of Dicer and the consequent down-regulation of canonical miRNA processing, thereby freeing miRNA processing and effector resources. The miR-144-

mediated repression of Dicer mediates this balance to promote the processing of pre-miR-451 during erythropoiesis.

DISCUSSION

Here we show that the Ago2-dependent processing of pre-miR-451 uncouples it from the biogenesis of Dicer-dependent miRNAs, facilitating the independent regulation of the two miRNA processing pathways and allowing miR-451 to evade the global miRNA down-regulation during erythropoiesis.

The evolution of the Ago2-dependent miRNA processing pathway has remained a mystery since its discovery. Contributing to the puzzle is the fact that this novel biogenesis pathway is strictly required for pre-miR-451 processing and terminal erythrocyte maturation across vertebrates. Our results indicate the existence of a negative feedback loop involving miR-144-mediated repression of Dicer which, together with other potential regulatory mechanisms (Wong et al., 2011), ultimately leads to a global canonical miRNA down-regulation during vertebrate erythropoiesis. The Ago2-dependent, Dicer-independent processing of miR-451 makes it refractory to the miRNA turnover and licenses it to become the most abundant miRNA in erythrocytes.

The uncoupling of miR-451 processing form the rest of canonical miRNAs allows the rise of independent regulatory mechanisms for each of the miRNA processing pathways. miR-451 is the only known example of Dicer-independent miRNA, but it would be interesting to know if the uncoupling of processing that allows alternative regulation of miRNA biogenesis is a common theme among other non-canonical miRNAs.

Despite diverging at the Dicer-cleavage step, both pathways still can compete for the availability of other miRNA processing and effector proteins, like PARN or Ago2, effectively linking their outcome. miR-451 represents an extreme case of 3'-to-5' miRNA trimming mediated by PARN (Yoda et al., 2013) but growing evidence indicates that canonical miRNAs are also substrate of PARN (Lee et al., 2019, Shukla et al., 2019). This is in concordance with our *in vivo* data, which suggests that miR-451 trimming is impaired when canonical miRNA levels increase (Figure 3H). In addition, miR-451 requires the slicer activity of Ago2 for its processing while the stability of mature miRNAs is directly proportional to the amount of Argonaute protein available (Diederichs and Haber, 2007). Although Ago2 is the most abundant Argonaute isoform in erythrocytes (Figure S6E), our results suggest that it is still expressed in limiting amounts, as Ago2 overexpression can

override the competition and increase the levels of mature canonical miRNA and miR-451 in fish embryos and mammalian cells (Figure 5E-H, S6C).

Ultimately, these cross-talks allow to maintain a concerted balance between both biogenesis pathways during erythropoiesis but also commit them to share the consequences of their demise. Our data show how in absence of miR-144 activity, canonical miRNAs increase but miR-451 trimming is impaired. On the opposite hand, reduction of Dicer activity increases miR-451 biogenesis at expense of canonical miRNAs, highlighting the exquisite equilibrium between both miRNA processing pathways.

miR-144 targeting Dicer affects canonical miRNA levels in erythrocytes

Individual microRNA biogenesis and turnover is known to be regulated by RNA-binding proteins and transcription factors (Treiber et al., 2019). Although we do not discard that these regulatory mechanisms, together with other chromatin regulators and transcription factors (Wong et al., 2011) also play an important role during erythropoiesis, the negative feed-back loop between miR-144 and Dicer has the advantage that it dampens the biogenesis of all canonical miRNAs expressed in blood simultaneously (Figure 6A and 6B).

Indeed, there are other examples of negative feedback loops regulating miRNA processing enzymes. For example, miR-103/107 target Dicer to promote epithelial-to-mesenchymal transition and increased expression of the cluster is associated with metastasis and poor prognosis in breast cancer (Martello et al., 2010). The same miR-107 targets Dicer in zebrafish to prevent excessive neurogenesis mediated by miR-9 (Ristori et al., 2015). In worms, miR-71 targets *alg-1*/Argonaute to induce a global miRNA regulation during aging (Inukai et al., 2018). The mechanism that we expose here is unique in the sense that it integrates the miR-144/Dicer regulatory loop with a Dicer-independent and Ago2-slicing-mediated miRNA processing pathway (Figure 6A and 6B) to establish a new regulatory layer in *trans* between clustered miRNAs.

miR-144 regulates miR-451 in trans

The data presented here supports the role of miR-144 regulating miR-451 in *trans.* By swapping the seed region of the miR-144 stem (Figure S6A), our experimental design avoids disturbing the secondary structure of the miR-144/451 cluster and any *cis* interaction is maintained which allows us to specifically interrogate *trans* effects between the two miRNAs in the cluster. Our results indicate that when the biogenesis of the miRNAs in a cluster is uncoupled in two different processing pathways, each miRNA has the potential to regulate *trans*-factors that would enhance or impair the processing of the

partner miRNA. miR-144/451 are the first example of cluster miRNAs regulated in *trans*, but we speculate that this mode of regulation may also occur in other miRNA clusters where one of the members is differentially regulated by an RNA-binding protein.

While the physiological reasons to favor the demise of canonical miRNAs to promote maximal miR-451 production remain to be solved, our analysis of individual miRNA zebrafish mutants provide valuable insight into the specific role of miR-144 and miR-451 in erythrocyte development and homeostasis. Our results uncover the molecular signature of miR-144 loss-of-function and its contribution to erythrocyte maturation.

In sum, our results help us to understand the singularity of miR-451 processing and its role in vertebrate erythropoiesis. Future research will address if the Dicer-independent processing of miR-451 evolved as a response to the miRNA turnover during erythropoiesis or the non-canonical processing licensed the erythrocytes to opt for a global dampening of miRNAs.

ACKNOWLEDGMENTS: We thank A. Grishok, M. Garcia-Marcos, N. Lau, R. Afasizhev, D. O'Carroll and L. Zon for discussions. We thank E. Lai for providing Dicer KO MEFs. We thank R. Afasizhev and I. Afasizheva for providing access to Typhoon biomolecular imager.

AUTHOR CONTRIBUTIONS: DAK and DC designed, performed and analyzed the experiments; SM performed computational analysis; IAW helped with phenotypic analysis; AMM helped with cell culture experiments and Western blots; AMS helped with small RNA cloning; and DC wrote the manuscript.

DECLARATION OF INTERESTS: The authors declare no competing interests.

FUNDING: Supported by NIH grants R00-HD071968-03 (DC), R01GM130935-03 (DC) and Peter Paul Professorship (DC).

FIGURE LEGENDS

Figure 1. Ago2-dependent miRNA processing is less efficient than Dicer-dependent processing. A) Schematic representation of Dicer-dependent and Ago2-dependent miRNA processing pathways. **B)** Histogram showing relative abundance of miRNAs in the blood of embryos 48 hpf. **C)** Secondary structure of different miR-451 precursors reprogrammed to be processed by Dicer or Ago2. Dotted rectangle indicates endogenous *Danio rerio* pre-miR-451. **D)** Northern blot analysis to detect the processing of Ago2- and Dicer-dependent pre-miRNAs. The sequences and secondary structures of the injected hairpins are shown in Figure 1C. **E)** The EYFP-2xIPT-miR-451 reporter (green) contains two imperfect target sites to miR-451 in its 3'UTR and was co-injected together with control TagRFP mRNA (red). Where indicated, the embryos were additionally injected with the wild-type pre-miR-451^{Ago2} hairpin (hairpin #1 in Figure 1C) or the pre-miR-451^{Dicer} hairpin (hairpin #4 in Figure 1C). **F)** Representative Northern blot showing a time course of the processing of Ago2- and Dicer-dependent pre-miR-451. Experiments were done in triplicate. **G)** Quantification of the amount of injected pre-miRNA cleaved in Figure 1F, calculated as the ratio of the intensity mature/(mature+precursor). Dots represent mean±SD of each triplicate.

Figure 2. miR-144-3p destabilizes *dicer1* mRNA and dampens the expression of canonical miRNAs. A) Predicted miR-144-3p target sites in *dicer1* 3'UTR of *Danio rerio*. miR-144-3p seed region is indicated in red. **B)** Luciferase reporter assays to validate miR-144 targeting of the *dicer1* 3'UTR. The reporter mRNA contains the Nanoluciferase (NLuc) ORF followed by the *Danio rerio dicer1* 3'UTR wild-type sequence or with the miR-144 sites mutated. Each reporter was co-injected with Firefly luciferase (Fluc) and with or without miR-144 duplex. NLuc activity was normalized to Fluc activity and its value for the control sample without miRNA duplex was set to 100%. Data represent average of four biological replicates (three for the sensor with mutant 3'UTR) performed on different days, with 5 independent replicates each day. ***: $p<0.0001$, ANOVA test. **C)** RT-qPCR of *dicer1* in wild-type and miR-144$^{\Delta/\Delta}$ showing that dicer mRNA is more abundant in blood from miR-144$^{\Delta/\Delta}$ mutants. Total RNA was isolated from peripheral blood of 2-day-old embryos. Expression of *dicer1* was normalized on *actin* mRNA levels. **: $p = 0.0056$, unpaired *t* test. **D)** MicroRNA sequencing of peripheral blood isolated from 2-day-old embryos. Reads were mapped to pre-miRNA hairpins and normalized with spike-ins.

Figure 3. Loss of miR-144 impairs erythrocyte maturation. A) Schematic representation of genomic deletions in miR-451$^{\Delta/\Delta}$ and miR-144$^{\Delta/\Delta}$ used in this study. **B)** Northern blot of endogenous miR-451 and miR-144 processing in wild-type, miR-451$^{\Delta/\Delta}$

and miR-144$^{\Delta/\Delta}$ at 48 hpf. **C)** Cumulative distributions of fold changes between wild-type embryos and miR-144$^{\Delta/\Delta}$ or miR-451$^{\Delta/\Delta}$ embryos for miRNA targets (orange and red lines) and non-targets (grey line). **D)** O-dianisidine staining of 2-day-old embryos to reveal the hemoglobinized cells. **E)** May-Grunwald Giemsa staining of peripheral blood isolated from adult wild-type, miR-144$^{\Delta/\Delta}$, miR-451$^{\Delta/\Delta}$ and Ago2$^{\Delta/\Delta}$ fish. **F)** Quantitative analysis of nuclear area and nuclear granularity from adult blood smears stained as in **E**. Nuclear granularity is measured with ImageJ as the average grey value of pixels in the nuclear area. Between 38 and 132 cells are analyzed in each case. Boxes enclose 5 to 95 percentiles. ****: $p<0.0001$, one-way ANOVA. **H)** Northern blot of endogenous miR-451 processing at 48 hpf in wild-type and miR-144$^{\Delta/\Delta}$ performed in triplicates. Red arrowheads pinpoint the bands corresponding to the intermediate trimming species accumulated in miR-144$^{\Delta/\Delta}$ mutants. **I)** Representative Northern blot analysis of endogenous miR-451 processing at 48 hpf in wild-type, miR-144$^{\Delta/\Delta}$ and miR-144$^{\Delta/\Delta}$ injected with synthetic miR-144 duplex. Red arrowheads pinpoint the bands corresponding to the intermediate trimming species accumulated in miR-144$^{\Delta/\Delta}$ mutants. Densitometry quantification of the bands is shown in Figure S4H. **J)** Northern blot analysis of miRNA levels in peripheral blood isolated from adult WT, miR-144$^{\Delta/\Delta}$, and Dicer$^{+/-}$ zebrafish.

Figure 4. Over-expression of Dicer impairs miR-451 processing in mammals. **A)** and **B)** A plasmid encoding the miR-144/451 locus from human was transfected into HEK293T and Dicer KO MEFs cells together with EYFP and wild-type or catalytically dead Dicer plasmids. Total RNA was extracted 2 days after transfection. **C)** Northern blot analysis to detect the processing of miR-451 in Dicer KO MEFs co-transfected with plasmids encoding EYFP, or active and catalytically dead Dicer. **D)** Western blot of endogenous Dicer, Ago and Actin in Dicer KO MEFs expressing wild-type or catalytically dead Dicer**.** **E)** Quantification of mature miRNA abundance in *dicer1*$^{-/-}$ MEFs and **F)** HEK293T cells from three independent transfections. miR-451 abundance is measured as the sum of the intensities of the 23 to 30 nt bands. miRNA abundance was normalized on U6 snRNA. Efficiency of miRNA processing in cells transfected with EYFP was set to 100%. Error bars represent standard error of the mean. ****: $p<0.0001$, one-way ANOVA test.

Figure 5. Ago2-over-expression rescues competition between Dicer-dependent and Ago2-dependent pathways. A) Plasmids encoding wild-type miR-144/451 locus or with mutated miR-144 seed were transfected into HEK293T cells together with EYFP or *Hs*Dicer with its full-length 3'UTR carrying three target sites for miR-144. Efficiency of miR-451 processing was quantified from three representative Northern blots and normalized on U6 snRNA and respect to the miR-451 processing in the EYFP control. Error bars

represent mean ± standard deviation. **B)** Northern blot analysis to detect the processing of miR-451 in HEK293T co-transfected with wild-type miR-144/451 or mutated miR-144/451 locus and EYFP or *Hs*Dicer with its full-length 3'UTR. **C)** Western blot showing decreased accumulation of FLAG-Dicer carrying its 3'UTR in HEK293T cells when co-transfected with plasmid encoding wild type miR-144 compared to plasmid encoding miR-144 with mutated seed. **D)** Quantification of FLAG-Dicer levels as shown in Figure 5C. Found individual experiments were used for quantification. Data represented as mean ± standard deviation. **E)** Plasmid encoding wild-type miR-144/451 locus was transfected into HEK293T cells with EYFP or Dicer encoding plasmids and co-transfected with MmAgo2. Efficiency of miR-451 processing was quantified from three representative Northern blots and normalized on U6 snRNA and respect to the miR-451 processing in the EYFP control. Error bars represent mean ± standard deviation. *: p=0.03, two-way ANOVA test. **F)** Northern blot analysis to detect the processing of miR-451 from miR-144/451 locus co-transfected with EYFP or *Hs*Dicer and with or without *Mm*Ago2 encoding plasmids. **G)** Western-blot for FLAG-*Hs*Dicer, endogenous Dicer, Ago and Actin in HEK293T cells co-transfected with plasmids encoding FLAG-*Hs*Dicer and *Mm*Ago2. **H)** Northern blot analysis to detect the processing of Ago2- and Dicer-dependent pre-miRNAs (#1 and #4 from Figure 1C) in zebrafish with and without Ago2 over-expression. Zebrafish Ago2 (*Dr*Ago2) and mouse (*Mm*Ago2) were compared. Total RNA was extracted 6 hours after injection. **I)** Western blot showing the overexpression of Ago2 in zebrafish embryos.

Figure 6. Mechanisms regulating microRNA biogenesis during erythropoiesis. A) Cartoon showing potential regulatory mechanisms that could orchestrate the turnover of all miRNA but one. Specific chromatin factors, transcription factors and RNA-binding proteins could act on each individual miRNA to regulate their expression and processing. Alternatively, down-regulation of Dicer by the negative feedback loop excerted by miR-144, together with other potential modes of regulation, can impair canonical miRNA processing globaly. miR-451 would evade this miRNA down-regulation by opting for an alternative Dicer-independent, Ago2-dependent miRNA processing pathway. **B)** During erythrocyte maturation, miR-144 represses Dicer in a negative feed-back loop, complementing other potential transcriptional regulation of Dicer. As a consequence of the repression of Dicer, canonical miRNAs are reduced and miR-451 biogenesis increases.

Figure 1

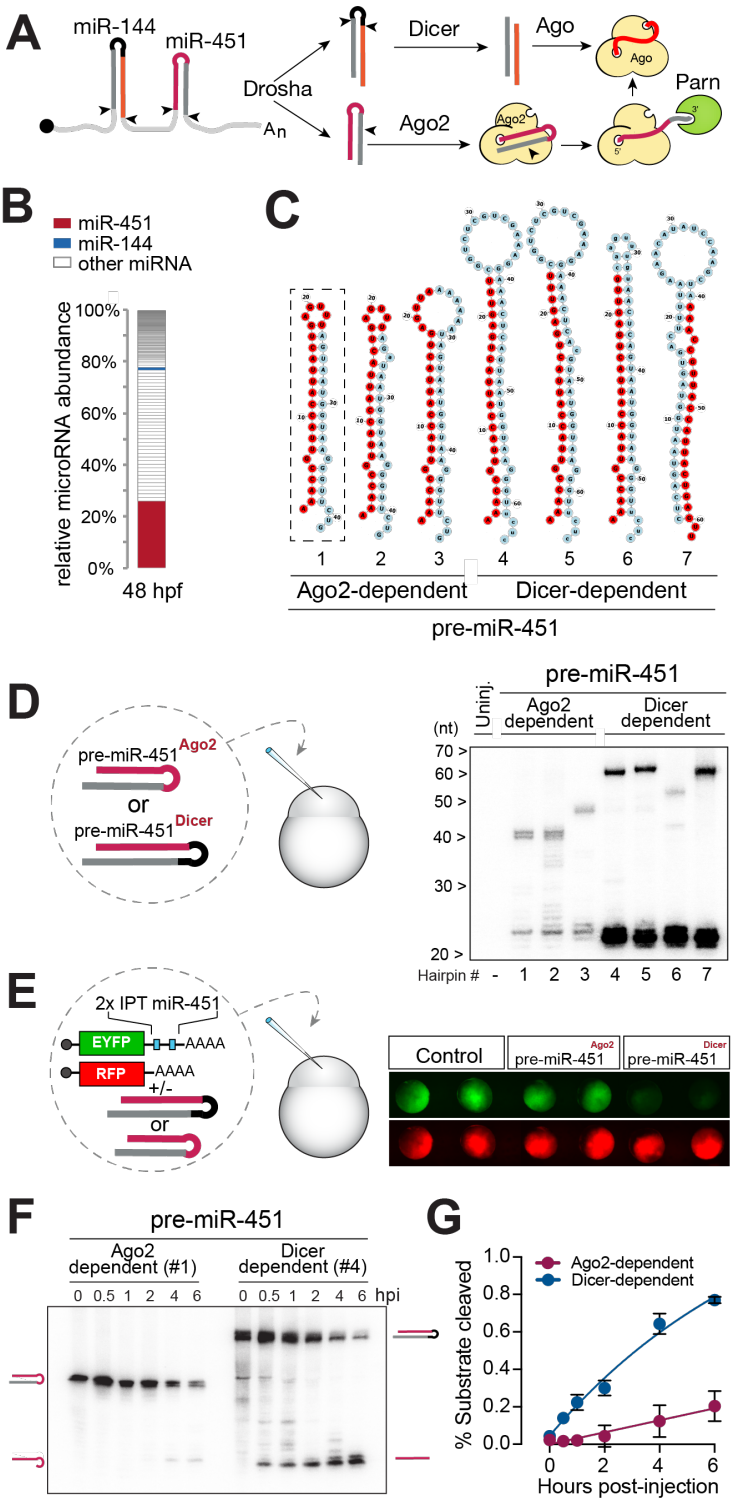

Figure 1. Ago2-dependent miRNA processing is less efficient than Dicer-dependent processing.

Figure 2

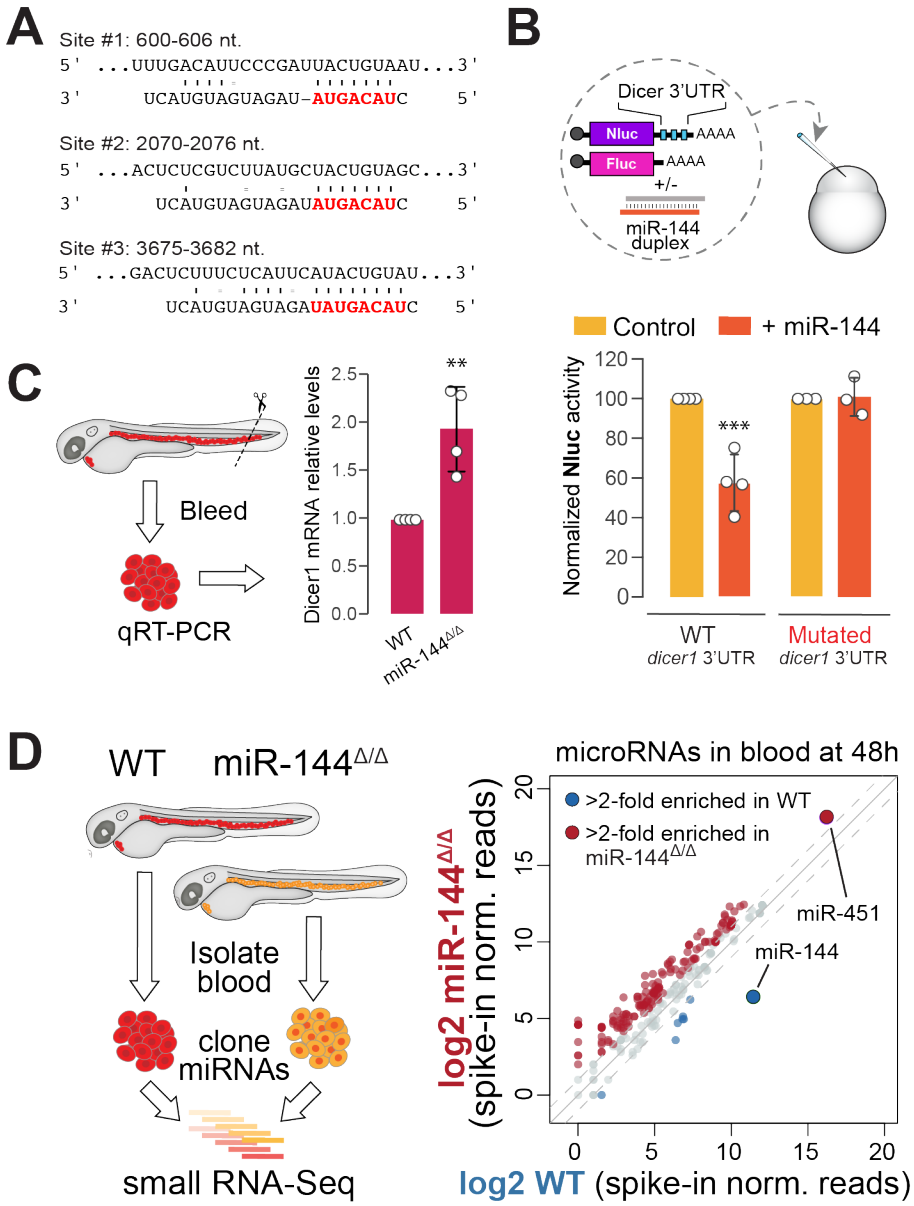

Figure 2. miR-144-3p destabilizes *dicer1* mRNA and dampens the expression of canonical miRNAs.

Figure 3

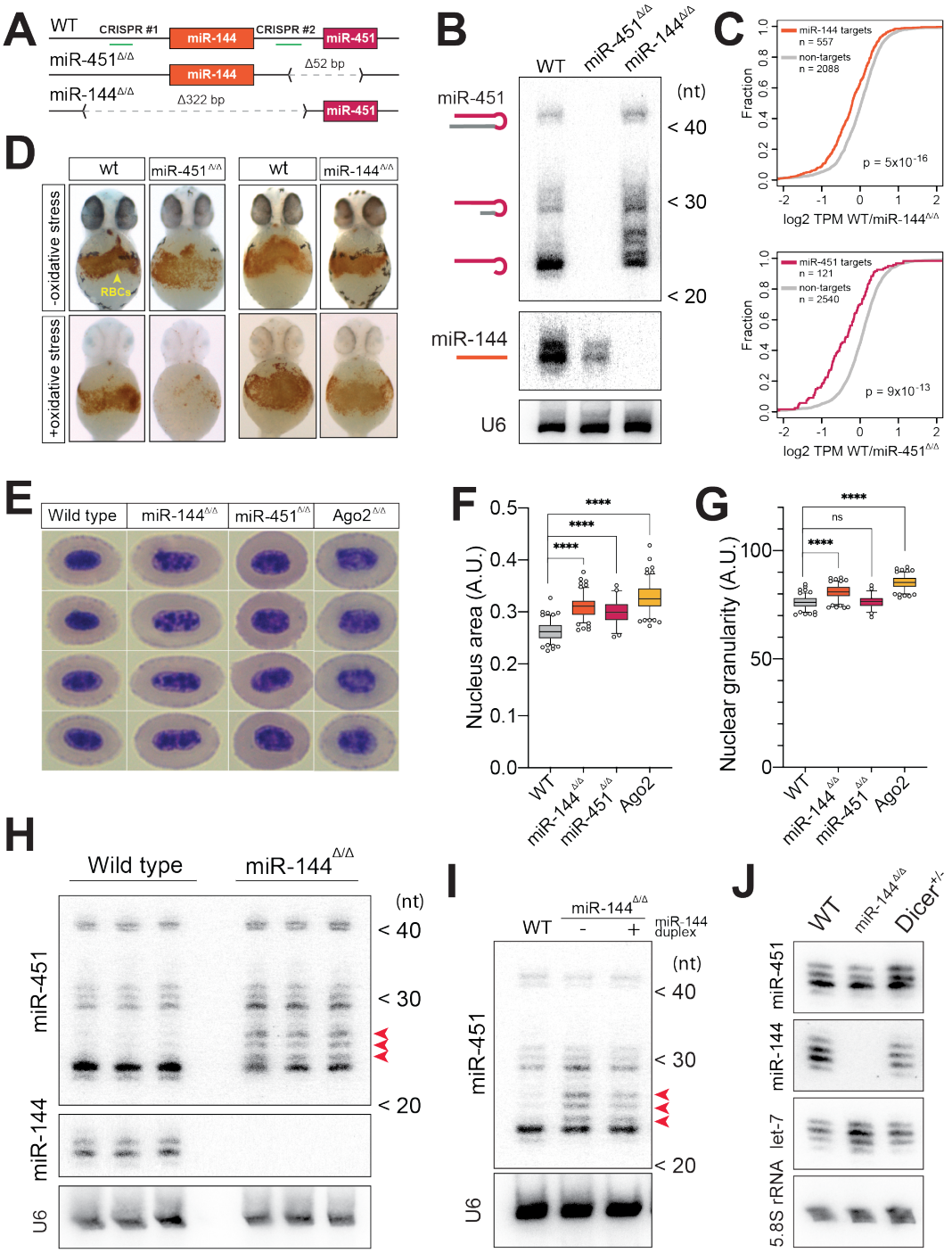

Figure 3. Loss of miR-144 impairs erythrocyte maturation.

Figure 4

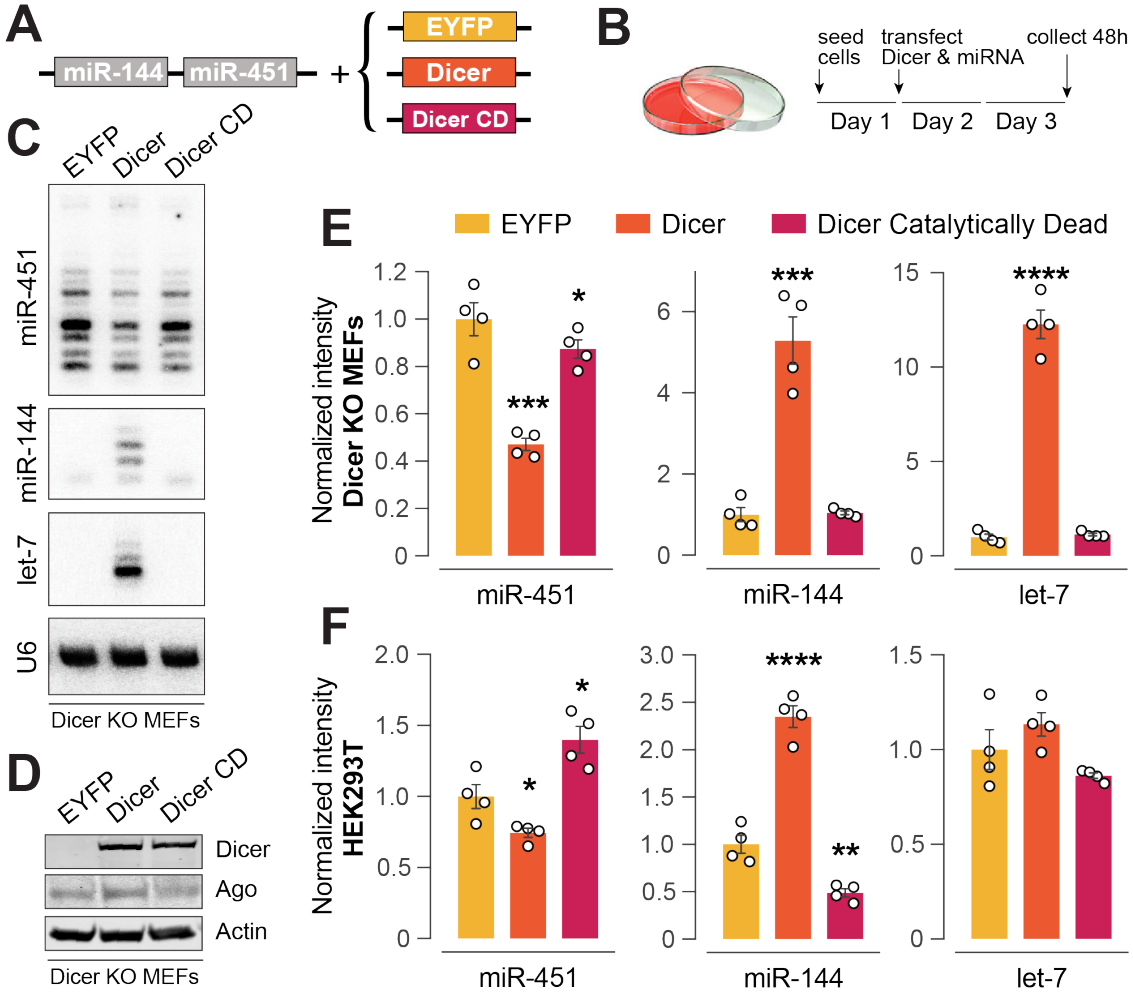

Figure 4. Over-expression of Dicer impairs miR-451 processing in mammals.

Figure 5

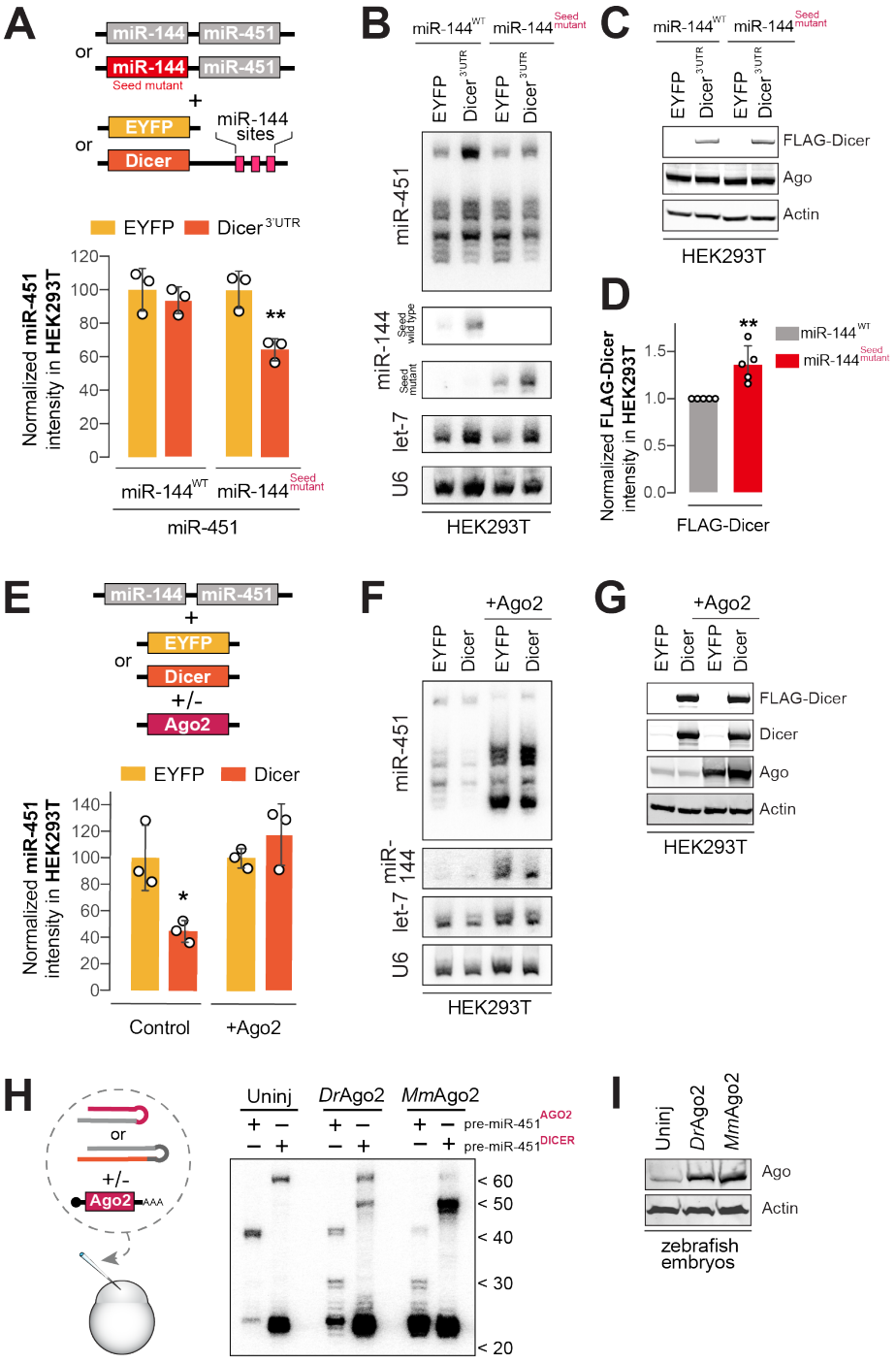

Figure 5. Ago2-over-expression rescues competition between Dicer-dependent and Ago2-dependent pathways.

Figure 6

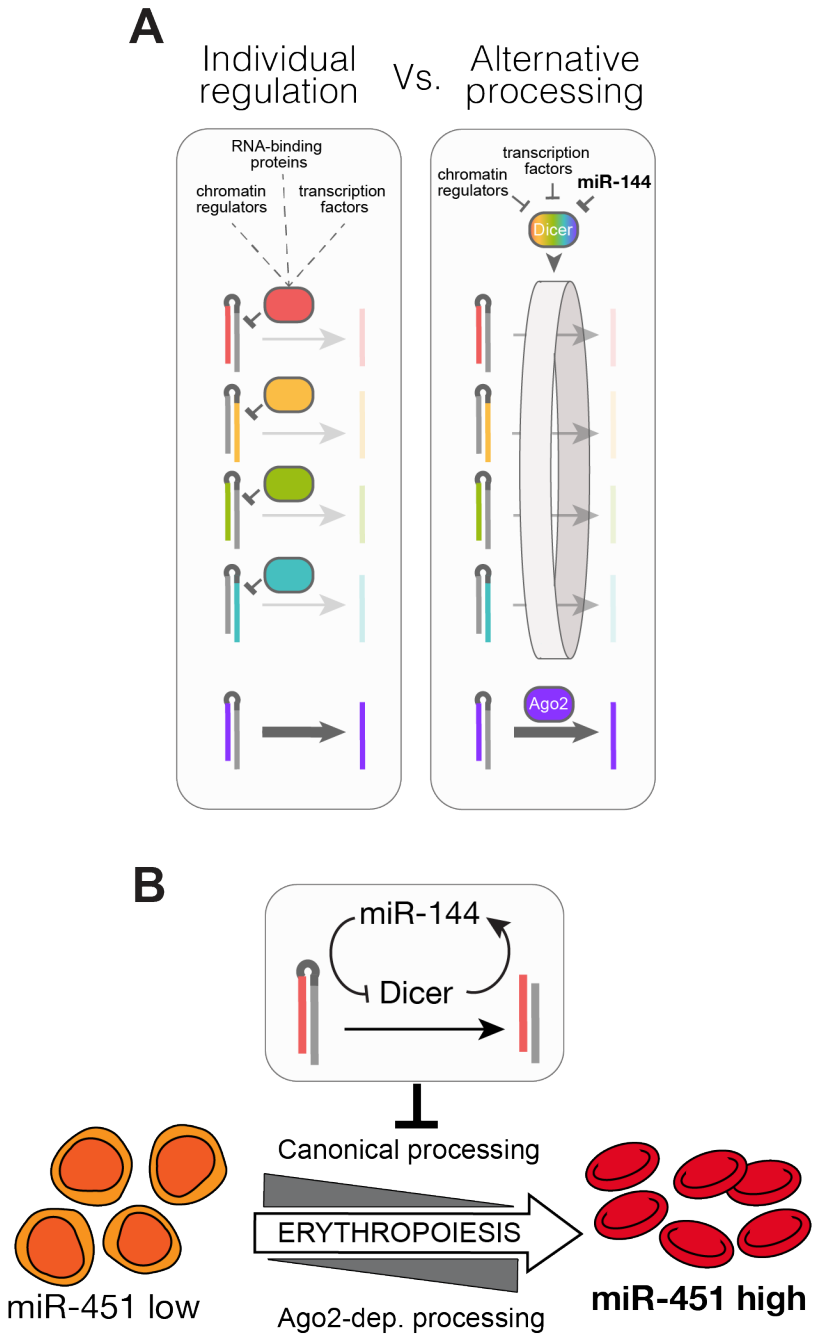

Figure 6. Mechanisms regulating microRNA biogenesis during erythropoiesis.

STAR METHODS

Zebrafish strains

Zebrafish strains were raised and maintained under standard laboratory conditions according to IACUC protocol (Animal protocol AN-5558) at Boston University. Experiments were conducted in hybrid wild-type strain crosses of AB/TU with TL/NIHGRI, in miR-451$^{\Delta/\Delta}$ and miR-144$^{\Delta/\Delta}$ mutant lines (generated in this study) and in Dicer$^{hu896/+}$.

Microinjections

Microinjections into embryos were performed as described previously (*1*). Briefly, zebrafish embryos were collected 15 min after fertilization and injected with glass needle at 1-cell stage into the animal pole. Needles were calibrated to inject the volume corresponding to 1 nL. After injections embryos were transferred into an agarose-coated 100 mm Petri dish and incubated at 28.5° C until processing.

Generation of miR-144/451 locus mutants using CRISPR/Cas9

sgRNAs surrounding miR-144 and miR-451 hairpins were designed using CRISPRscan (Moreno-Mateos, Nature Methods, 2015) yielding the following target sequences: Site #1 :5'- GGGGGTCAACGAGCCTCTGA(CGG)-3'; Site #2: 5'- GTTTCTGAAACTTTTGACAG(TGG)-3'; where the Cas9 PAM sequence (NGG) is between parentheses. sgRNA templates were generated by annealing and polymerase-mediated extension of a forward oligo containing the T7 promoter sequence, the 20 nt sgRNA target sequence (without the PAM sequence) and a 15 nt sequence complementary to the reverse oligo containing the invariable Cas9-binding scaffold. PCR reactions with Q5 high fidelity polymerase (New England Biolabs) were carried out as follows: 1 cycle 95°C for 3 minutes; 35 cycles (95°C for 3 minutes, 45°C for 30 seconds, 72°C for 20 seconds); 1 cycle at 72°C for 5 minutes. Reactions were purified with a PCR purification kit (New England Biolabs). Approximately 120–150 ng of DNA were used as a template for a T7 *in vitro* transcription (IVT) reaction with the AmpliScribe-T7- Flash transcription kit (Epicentre ASF3507). IVT sgRNA products were purified (Qiagen 74104) and quantified. Zebrafish embryos were injected at one-cell stage with *Cas9* mRNA (100 pg) together with sgRNA.1 and sgRNA.2 to generate miR-144$^{\Delta/\Delta}$ mutant and sgRNA.2 and sgRNA.3 to generate miR-451$^{\Delta/\Delta}$ mutant (30 pg of each sgRNA).

Cell culture and transfection

Dicer1$^{-/-}$ MEFs were kindly provided from Dr. Eric Lai. HEK293T and *dicer1*$^{-/-}$ MEF cell

lines were passaged in DMEM high glucose media (4.5 g/L) containing 10% FBS, 1% non-essential amino acids, 1% sodium pyruvate, penicillin/streptomycin, L-glutamate. Transfection was performed using Lipofectamine 3000 (Invitrogen). For each well of a 6-well plate, 2 mg of miRNA expression plasmid and Dicer or Argonaute expression constructs were transfected into the cells at 60% confluency. 48 h after transfection, cells were washed twice with 1X PBS. Total RNA was extracted with Trizol (Invitrogen).

Plasmid construction

All plasmids generated for this study are listed in Table S1. Genes of interest were amplified by PCR with the corresponding oligonucleotide pairs (Invitrogen) listed in Table S1. All cloning reactions were performed using NEBuilder® HiFi DNA Assembly Cloning Kit (New England Biolabs).

Small RNA Northern blotting

To detect miRNAs, a total of 20 (injected miRNAs) or 40 (endogenous miRNA) embryos were collected at the indicated time points. For HEK and Dicer KO MEFs cells input amount of total was 10 µg of total RNA. Total RNA was extracted using Trizol (Invitrogen) and resuspended in formamide. Loading buffer 2X (8 M urea, 50 mM EDTA, 0.2 mg/ml bromophenol blue, 0.2 mg/ml xylene cyanol) was added and the samples were boiled for 5 min at 95°C. miRNAs were separated in 15% denaturing urea polyacrylamide gel in 1X TBE and than were transferred to a Zeta-Probe blotting membrane (Bio-Rad) using a semi-dry Trans-Blot SD (Bio-Rad) at 20 V (0.68A) for 35 min. Membranes were UV cross-linked and pre-hybridized with ExpressHyb Hybridization Solution (Clontech) for 1 h at 50° C. Membranes were blotted with 5' ^{32}P-radiolabelled DNA oligonucleotide probes at 30°C overnight. Membranes hybridized with oligonucleotide DNA probes where washed at room temperature with 2x SSC/0.1% SDS followed by 1X SSC/0.1% SDS for 15 minutes. The blots were exposed to a phosphorimaging screen for 1 to 3 days. Signal was detected using the Typhoon FLA 7000 phosphorimager (GE Healthcare Life technologies) and analyzed using the ImageQuant TL software (GE Healthcare).

Preparation of radiolabeled probes

Radiolabeled DNA probes were prepared according to the StarFire method. Briefly, oligos carrying specific DNA sequence were annealed to the universal oligo (5'-TTTTTTTTTT666G6(ddC)-3', where “6” corresponds to a propyne dC modification) via complementary hexamer sequence. Annealed duplexes are then labeled with α-^{32}P-dATP in (6 µL of 10mCi/mL stock) the presence of the Klenow fragment of DNA polymerase. In

the presence of the Klenow fragment of DNA polymerase, radiolabeled α-^{32}P-dATP is "filled in" on the oligo-dT template of the universal oligo. Reaction was stopped by adding 40 µL of 10 mM EDTA solution to 10 µL of reaction . Then labeled oligos were purified using Micro-Spin G25 columns (GE HealthCare). Then 3,000,000 cpm of the P3[2] labeled StarFire probes were added to the membrane. Probe sequences used in this study are listed in Table 1.

microRNA processing assay

Pre-miRNA hairpins (IDT) (1 nL of 4 µM stock) were injected into single-cell stage zebrafish embryos together 1 nl of 0.2 mg/ml a-amanitin. Zebrafish (dreAgo2) and mouse (*Mm*Ago2) Ago2 mRNAs were *in vitro* transcribed using mMESSAGE mMACHINE SP6 Transcription Kit (Ambion) and then 100 nM was injected together with pre-mRNAs. Total RNA was extracted at 7 h after injection from 20 embryos and processing was analyzed by Northern blotting. For primary transcripts (pri-miRNAs), 1 nL of 1 µM stock was injected together 1 nl of 0.2 mg/ml a-amanitin. Total RNA was extracted at indicated time points.

Dicer Immunoprecipitation

mRNAs encoding for FLAG-tagged dreDicer1 was injected into single-cell stage zebrafish embryos (1 nL of 0.1 µg/µL stock) together with pre-miR-451 (1 nL of 10 µM stock). 100 embryos were collected 7 h after injection from each sample and washed twice with 1X PBS. The embryos were lysed with 500 µL of NET-2 buffer (100 mM Tris-HCl pH 7.5, 150 mM NaCl, 0.05% NP-40) and 1 µL of RNaseOUT (New England Biolabs) and protease inhibitor (Roche). Lysates were cleared by centrifugation at 16,000 x g. 50 µl of supernatant was kept as input and the rest of the was added to 500 µL of NET-2 with 50 µl of FLAG M2 magnetic beads (Sigma) and incubated for 2 h at 4°C. 50 µL of supernatant was removed for further analysis. The beads were washed 3 times with 500 µL of NET-2 buffer. 500 µL of Trizol (Invitrogen) was added to the beads to extract total RNA.

MicroRNA reporter assay

Full length Dicer 3' UTR from zebrafish was cloned into pCS2+ after coding sequence of NanoLuciferase or EYFP. Reporter constructs were linearized with NotI restriction enzyme and *in vitro* transcribed with mMESSAGE mMACHINE SP6 Transcription Kit (Ambion). For the fluorescent miRNA reporter assay, zebrafish embryos were injected with 1 nL of 100 ng/µL of EYFP-*Dre*Dicer 3'UTR reporter together with DsRed as a control reporter. Synthetic RNA oligonucleotides (IDT) representing the miR-451 and miR-144 duplex were annealed by incubation in 1X TE buffer at 90° C for 5 min and then slow cooled to room temperature. 1 nL of 10 µM miR-144 duplex was injected together with reporters. Embryos

were imaged for EYFP and DsRed expression at 8 h or 24 h after injection using a Zeiss Discovery microscope and photographed with a Zeiss Axiocam digital camera. Images were processed with ZEN software (Zeiss) and Photoshop CC19.16. For Nanoluciferase reporter groups of 5 embryos were collected 7 hours post-injection in triplicates or quintuplicates and lysed in 100 µL of Lyses buffer (Promega). Reporter expression was quantified with the Nano-Glo Dual-Luciferase Reporter Assay System (Promega) Synergy H1 Hybrid Multi-Mode Microplate Reader (Thermo).

Red blood cell isolation

Peripheral red blood cells from 48 h post-fertilization zebrafish embryos were isolated by dissection of caudal vein using sapphire blade in the collection buffer (1X PBS, 0.5 mM EDTA and 2% FBS. For small RNA-Seq and RNA-Seq experiments collection buffer without serum was used instead and cells were collected directly into Trizol. Peripheral blood from adult zebrafish embryos was isolated from WT, miR-144-/- and Dicer$^{+/-}$, zebrafish by collecting blood from cut fin of adult fish in 1X PBS containing 2% PBS and 5 mM EDTA. 1 µg of total RNA was used for Northern blot analysis.

Small RNA library preparation

Small RNA libraries were prepared from total RNA (0.5 µg) isolated from peripheral blood of wild type and miR-144$^{\Delta/\Delta}$ embryos at 48 hours post-fertilization. Small RNAs were size-selected in 10% denaturing polyacrylamide gel in 1X TBE in range from 18 to 75 nucleotides. RNA extraction from the gel was achieved by incubation in 0.3 M NaCl overnight at 4°C with following precipitation with isopropanol. Pre-adenylated 3' custom adaptor was ligated to small RNAs by T4 RNA ligase for 2 h at 22° C. After ligated products were size-selected by gel from non-ligated adaptor. Reverse transcription was performed by SuperScript III Reverse Transcription kit (Thermo Fisher) using RT Cloning Primer. Then cDNA products were isolated by gel selection and then circularized by CircLigase ssDNA Ligase (Epicentre). cDNA libraries were amplified in reactions containing forward and reverse Illumina index primers. Oligo sequences and reagents used for library preparation are provided in the Key Resource table.

mRNA library preparation

mRNA libraries were cloned from polyA(+) RNA isolated from isolated from peripheral blood of 2-day-old WT, miR-144$^{\Delta/\Delta}$ and miR-451$^{\Delta/\Delta}$ zebrafish embryos according to Illumina TruSeq protocol. Libraries were cloned and sequenced at Boston University Microarray

and Sequencing core.

Small RNA Sequencing data analysis

FASTQ files were split by barcode into respective samples. The first 5 nucleotides of each sequence were trimmed. These 5 clipped nucleotides include the 4 degenerate nucleotides added in the 5' adapter to avoid ligation bias and the first nucleotide of the insert, as it has the potential to be a non-templated nucleotide added during the retrotranscription step. At the 3' end, we removed the 4-nucleotide custom barcode (wt: CACA; miR-144$^{\Delta/\Delta}$: AGAG) and preceding two bases that correspond to degenerate nucleotides added to avoid ligation bias. Reads were mapped to zebrafish pre-miRNA hairpins from miRBase (v22.0) using PatMaN with zero mismatches or gaps allowed. Spike in reads were counted in each sample using a custom Perl script. Raw counts of the sum of reads aligning to each miRNA hairpin were scaled relative to total spike in counts in each sample.

mRNA-Seq Sequencing data analysis

Transcript based counts were obtained from Kallisto (v0.44.0) using *Danio rerio* GRCz10 cDNA annotation downloaded from Ensembl. Sleuth (v0.29.0) was used for between sample normalization and to calculate aggregate gene counts.

May-Grunwald Giemsa staining

RBCs from adult zebrafish embryos were isolated from WT, miR-144-/- and miR-451-/- zebrafish by collecting blood from cut fin of adult fish in 1X PBS containing 2% PBS and 5 mM EDTA. RBCs were spread on Superfrost Plus microscope slides using StatSpin Cytofuge (Beckman) at 1,000 rpm for 4 min. Then cells were fixed in iced cold methanol for 5 min and air-dried. Cells were incubated for 5 min in May-Grünwald Stain (Sigma). After slides were rinsed twice in 1X PBS in transferred into dilute Giemsa solution (1:20) (Sigma) for 20 min. Finally, briefly rinsed in deionized water and air-dried (Sigma). Slides were mounted using ProLong Gold Antifade Reagent (Life Technologies).

O-dianisidine staining

Hemoglobin was detected in 48 h post-fertilization embryos by incubation for 15 min in the dark in O-dianisidine staining solution (0.62 mg/ml O-dianisidine, 0.65 H_2O_2, 40% ethanol and 10mM sodium acetate) and then transferred into 1X PBS. To apply oxidative stress, live embryos were transferred to water containing 0.003% phenylthiourea (PTU) from 8 hpf until collection time at 48 hpf.

cDNA Preparation and qPCR

cDNA was prepared from total RNA (0.5 µg) by reverse transcription using SuperScript III Reverse Transcription kit (Thermo Fisher) using random hexamer primer. qPCR reactions were performed using Power SYBR Green Master Mix (Thermo) and carried in ViiA7 Real-Time PCR System (Applied Biosystems) and analyzed using the ddCT method. Data were normalized to *Actb* amplification.

Western-blotting

The HEK293T cell or MEF Dicer-/- cells were collected from 6-well plates by scrapping 2 days after transfection in 1X PBS and resuspended in 100 µL of IPH lysis buffer (50 mM Tris-HCL pH 8.0, 250 mM NaCL, 5 Mm EDTA, 1% NP-40 and supplemented with Protease inhibitor cocktail (Roche)). Cells were incubated on ice for 20 min and then centrifuged for 10 min at 21,000g at 4°C. Supernatant was collected and protein concentration was measured by Bradford assay (BioWorld) using Ultraspec 2100 pro spectrophotometer (Amersham Biosciences). 20 to 40 µg of total protein was mixed with 1x LDS Sample buffer and Sample Reducing Agent (NuPAGE™) and incubated 5 min at 95°C.

To extract proteins from zebrafish embryos deyolking procedure was applied. Briefly, 100 embryos were resuspended in 200 µL deyolking buffer (55 mM NaCL, 1.8 mM KCl, 1.25 mM $NaHCO_3$) and incubated for 5 min at 1,100 rpms at 4°C. Then, cells were pelleted by centrifugation for 30 sec at 300g at 4°C. Then they were washed twice with Wash Buffer (110 mM NaCl, 3.5 mM KCl, 2.7 mM $CaCl_2$, 10 mM Tris-HCl), pH 8.5). Finally, cell pellet was resuspended in 1X LDS Sample buffer supplemented with Reducing Agent and incubated for 5 min at 95°C.

Proteins were resolved using precast NuPAGE Novex 8% Bis-Tris gel plus (Invitrogen) at room temperature and constant voltage (100 V) in 1X MOPS Running buffer and transferred to a nitrocellulose membrane (0.45 µM, Bio-Rad) using wet transfer (NuPAGE 1X transfer buffer supplemented with 10% of Methanol) overnight at 4°C and constant voltage (10V). After transfer membranes were blocked in a blocking buffer (5% non-fat dry milk in TBS-T) for 1 hour at room temperature. Membranes were incubated with primary antibody overnight at 4°C with following dilutions. Anti-Dicer (1:1000), anti-FLAG (1:1000), anti-Ago (1:1000), anti-actin (1:1000).

After that membranes were washed three times with TBS-T and then incubated with secondary antibody for 2 h at room temperature with following dilutions. IRDye 800CW Goat anti-mouse (1:10000), IRDye 680RD Goat anti-rabbit (1:10000). All membranes were scanned using Oddysey Scanner (Li-COR) and band intensity was quantified with Oddysey software.

SUPPLEMENTARY FIGURE LEGENDS

Figure S1. Related to Figure 1.

(A) Quantification by Northern blot of miR-451 and **(B)** miR-144-3p amounts in 48 h old WT embryos and in red blood cells (RBCs) isolated form adult zebrafish. The calibration curve was plotted by measuring the signal from synthetic miR-451 and miR-144-3p loaded into the gel at known concentrations. Each Northern blot was performed in triplicates. Bars indicate mean ± standard deviation. **C)** Time course analysis by Northern blot of the processing of miR-451 and miR-144 from wild-type or reprogrammed pri-miR-144/451 primary transcripts. Reprogrammed transcript encodes Dicer-dependent miR-451 corresponding to the hairpin #4 from Figure 1C). **D)** Quantification of pre-miRNA and mature miR-451 levels from S1C. Each Northern blot was performed in triplicates. Bars indicate mean ± standard deviation. **E)** Analysis of the change in miRNA expression between CFU-E erythroid progenitors and Ter119+ mature erythroblast cells from (Zhang et al., 2011). **F)** Re-plotting of the data from Figure S1E as a histogram, showing relative abundance of miRNAs in mouse CFU-E erythroid progenitors and Ter119+ mature erythroblasts.

Figure S2. Related to Figure 2.

A) Quantification by mass-spectroscopy of Dicer1 and Ago2 levels during human erythroid differentiation (adapted from Gautier et al, 2016, Cell Reports). **B)** Predicted 7 or 8mer miR-144-3p target sites in the *dicer1* 3'UTR of vertebrates according to TargetScan 7.2. For human *dicer1* 3'UTR, we included a manually annotated 6mer site. miR-144-3p seed region is indicated in red.

Figure S3. Related to Figure 2.

A) EYFP reporter mRNA (green) was co-injected at the one-cell stage with control TagRFP mRNA (red). The EYFP reporter contains the full 3'UTR of *dicer1* from *Danio rerio* and was co-injected together with miR-144 duplex. **B)** Nanoluciferase (Nluc) reporter assays to validate miR-144 targeting of the human *dicer1* 3'UTR. Reporter was co-transfected with Firefly luciferase (Fluc) and with control or miR-144 duplex. Nluc activity was normalized to Fluc and its value for the control sample without miRNA duplex was set to 100%. Data represent average of three biological replicates performed on different days, with 3 independent replicates each day. ***: $p<0.0005$, unpaired t test. **C)** Northern blot analysis of miR-451, miR-144, miR-223 and miR-16 processing during the time course

of zebrafish development in WT and miR-144$^{\Delta/\Delta}$. **D)** Northern blot analysis of miR-144 and miR-451 processing from the RNA precursors (corresponding to WT, miR-144$^{\Delta/\Delta}$ and miR-451$^{\Delta/\Delta}$) injected into singe stage embryos. Total RNA was extracted at 8 hpf.

Figure S4. Related to Figure 3.

A) Bright-field microscopy of 30 h post fertilization WT, miR-144$^{\Delta/\Delta}$ and miR-451$^{\Delta/\Delta}$ embryos. **B)** Expression of hemoglobin is visualized by O-dianisidine staining at 48 hpf in wild-type and miR-451$^{\Delta/\Delta}$ embryos in normal conditions and upon oxidative stress induced by incubation with 0.003% phenylthiourea. This figure includes the wild type and miR-451$^{\Delta/\Delta}$ embryos from Figure 3D plus additional siblings for comparison and to show reproducibility **C)** O-dianisidine staining of 2-day-old wild-type or miR-451 mutant embryos rescued with synthetic miR-451 duplex. **D)** Same as Figure S4B, but this time comparing wild-type and miR-144$^{\Delta/\Delta}$ embryos. This figure includes the wild type and miR-144$^{\Delta/\Delta}$ embryos from Figure 3D plus additional siblings for comparison and to show reproducibility. **E)** Scatter plot of mRNA-Seq data showing that there is no change in PARN expression in miR-144$^{\Delta/\Delta}$ compared to wild type in peripheral blood isolated from 2-day-old zebrafish**. F)** Cumulative distributions of fold changes between wild-type embryos and miR-144$^{\Delta/\Delta}$ or miR-451$^{\Delta/\Delta}$ embryos for miR-451 and miR-144 targets, respectively (red and orange lines) and non-targets (grey line). p-values are calculated using Wilcoxon rank-sum test. **G)** RT-qPCR of *pre-miR-144/451* transcript in miR-144$^{\Delta/\Delta}$ and miR-451$^{\Delta/\Delta}$ embryos relatively to its levels in wild type siblings. Total RNA was isolated from forty 2-day-old embryos per replicate and five independent replicates were performed for each genotype. Expression of *pri-miR-144/451* in wild type, miR-144$^{\Delta/\Delta}$ and miR-451$^{\Delta/\Delta}$ mutants was normalized to *actin* mRNA levels in each experiment. **H)** Plot profile showing density distribution of different products of pre-miR-451 processing showed in Fig 3I. **I)** Northern blot of endogenous miR-144 accumulation at 48 hpf in wild-type, miR-451$^{\Delta/\Delta}$, and miR-451$^{\Delta/\Delta}$ injected with synthetic miR-451 duplex. **J)** Northern blot analysis of miRNA levels in peripheral blood isolated from adult wild type and miR-451$^{\Delta/\Delta}$ zebrafish.

.

Figure S5. Related to Figure 4.

A) Northern blot analysis to detect the processing of miR-451, miR-144-3p and let-7 in HEK293T cells co-transfected with plasmids encoding EYFP, or active and catalytically dead human Dicer. **B)** Western-blot for FLAG-Dicer, endogenous Dicer, Ago and Actin in HEK293T cells expressing wild-type or catalytically dead Dicer**.**

Figure S6. Related to Figure 5

A) pri-miRNA structure of miR-144 wild-type and 3'-arm seed mutant. Nucleotides in red indicated the mutation site. Structures were calculated using RNAfold and visualized using Forna. **B)** Immunoprecipitation of FLAG-*Dre*Dicer from wild-type embryos injected with Ago2- and Dicer-dependent pre-miR-451 followed by Northern blot analysis to detect bound miR-451. Supernatant (S), and immunoprecipitate (IP) are indicated. **C)** Northern blot analysis to detect the processing of miR-451, miR-144-3p and let-7 in Dicer KO MEFs co-transfected with GFP or human Dicer in the presence of catalytically active Ago2. U6 was used as normalization control in all pre-miRNA processing experiments. **D)** Western-blot for FLAG-*Hs*Dicer, endogenous Dicer, Ago and Actin in Dicer KO MEFs co-transfected with plasmids encoding FLAG-*Hs*Dicer and *Mm*Ago2**. E)** RPKM of Argonaute paralogues in peripheral blood from 2-day-old embryos.

Figure S1. Related to Figure 1.

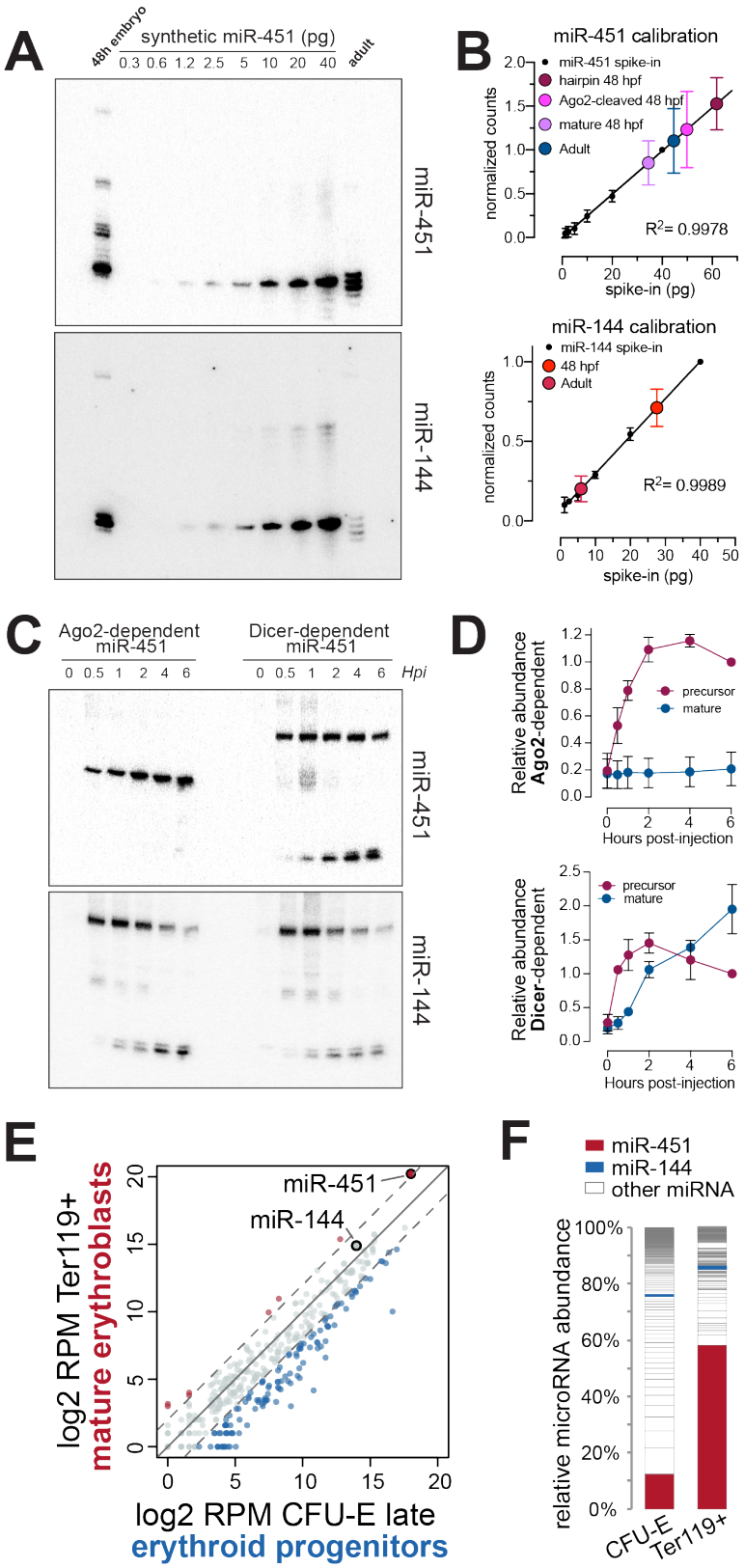

Figure S2. Related to Figure 2.

A

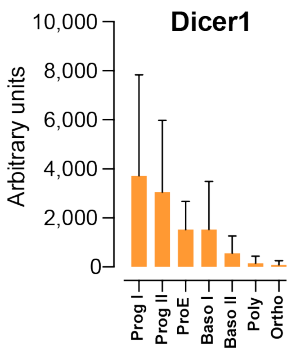

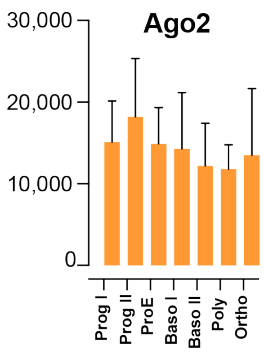

Prog I: Burst-forming units-erythroid
Prog II: Colony-forming units-erythroid
ProE: Proerythroblasts
Baso I: Basophilic I
Baso II: Basophilic II
Poly: Polychromatophilic erythroblasts
Ortho: Orthochromatic erythroblasts

B

miR-144-3p targets in HUMAN *dicer1* 3'UTR

Site #1: 7mer-m8 635-641
also conserved in Rhesus and Chimp
5'...UUUUCUUUCCACGUUAUACUGUG...3'
3' GAUCAUGUAGUAGAU**AUGACA**U 5'

Site #2: 7mer-m8 1779-1785
also conserved in Rhesus,Chimp, Cow, Cat, Dog, Brown bat, Opossum, Macaw, Chicken
5'...GUAAGUGACAUUUGA-AUACUGUC...3'
3' GAUCAUGUAGUAGAU**AUGACA**U 5'

Site #3: 6mer 3193-3198
5' ...UUGUCUGUGGCAUUUUUACUGUUU...3'
3' UCAUGUAGUAGAU**AUGACA**U 5'

miR-144-3p targets in RHESUS *dicer1* 3'UTR

Site #1: 8mer 647-654
also conserved in Rhesus, Human and Chimp
5'...UUUUCUUUCCAUGUU--AUACUGUA...3'
3' UCAUGUAGUAGAU**AUGACA**U 5'

Site #2: 7mer-A1 1261-1267
also conserved in Cat, Macaw, Chicken and Lizard
5'...CUCACAUAAAUUUCUUACUGUAC...3'
3' UCAUGUAGUAGAU--**AUGACA**U 5'

Site #3: 7mer-m8 1802-1808
also conserved in Human, Chimp, Cow, Cat, Dog, Brown Bat,Opposum, Macaw, Chikcen
5'...GUAAGUGACAUUUGA-AUACUGUC...3'
3' UCAUGUAGUAGAU**AUGACA**U 5'

miR-144-3p targets in CHIMP *dicer1* 3'UTR

Site #1: 7mer-m8 635-641
also conserved in Human, Rhesus
5'...UUUUCUUUCCACGUUAUACUGUG...3'
3' GAUCAUGUAGUAGAU**AUGACA**U 5'

Site #2: 7mer-m8 1779-1785
also conserved in Human, Rhesus, Cow, Cat, Dog, Brown Bat, Opossum,Macaw, Chicken
5'...GUAAGUGACAUUUGA-AUACUGUC...3'
3' GAUCAUGUAGUAGAU**AUGACA**U 5'

miR-144-3p targets in COW *dicer1* 3'UTR

Site #1: 8mer 1818-1825
also conserved in Human, Chimp, Rhesus, Cat, Dog, Brown Bat,Opposum, Macaw, Chicken
5'...UUGAAUUGCAGUCGAAUACUGUA...3'
3' GAUCAUGUAGUAGAU**AUGACA**U 5'

miR-144-3p targets in DOG *dicer1* 3'UTR

Site #1: 8mer 1875-1882
also conserved in Human, Chimp, Rhesus, Cat, Cow, Brown Bat,Opposum, Macaw, Chicken
5'...UUACAUUACAGUGGA-AUACUGUA...3'
3' GAUCAUGUAGUAGAU**AUGACA**U 5'

Site #2: 7mer-m8 3467-3473
5'...AAAUACUAAUAUAUUAUACUGUU...3'
3' GAUCAUGUAGUAGAU**AUGACA**U 5'

Site #3: 8mer 4335-4342
5'...GCUGUUCUAAGGAACAUACUGUA...3'
3' GAUCAUGUAGUAGAU**AUGACA**U 5'

miR-144-3p targets in MOUSE *dicer1* 3'UTR

Site #1: 7mer-m8: 2208-2214
also conserved in Rat
5'...UAACUAGUUUGAAUCAUACUGUGA...3'
3' UCAUGUAGUAGAU**AUGACA**U 5'

miR-144-3p targets in OPOSSUM *dicer1* 3'UTR

Site #1: 8mer 1762-1769
also conserved in Human, Chimp, Rhesus, Cow, Cat, Dog, Brown bat, Macaw, Chicken
5'...UUAACUCACAAGUGAAUACUGUA...3'
3' GGUCAUGUAGUAGAU**AUGACA**U 5'

Site #2: 8mer 4247-4254
also conserved in Macaw, Chicken, Lizard, X. tropicalis
5'...AAAUGUAAUUCAUUCAUACUGUA...3'
3' GGUCAUGUAGUAGAU**AUGACA**U 5'

Site #3: 8mer 2856-2863
also conserved in Macaw, Chicken, Lizard
5'...AAUUUUUUCUUAUUUAUACUGUA...3'
3' GGUCAUGUAGUAGAU**AUGACA**U 5'

Site #4: 8mer 3763-3770
also conserved in Rat
5'...GAAUUCCUUUAUUUUAUACUGUA...3'
3' GGUCAUGUAGUAGAU**AUGACA**U 5'

Site #5: 7mer-m8 687-693
5'...AAUGGCUGGGCUGGCAUACUGUU...3'
3' GGUCAUGUAGUAGAU**AUGACA**U 5'

Site #6: 7mer-m8 2720-2726
5'...AGUGUUGAGCAGAAAAUACUGUU...3'
3' GGUCAUGUAGUAGAU**AUGACA**U 5'

miR-144-3p targets in RAT *dicer1* 3'UTR

Site #1: 7mer-m8 2351-2357
also conserved in Mouse
5'...CCCACAGUUUGAAUCAUACUGUG...3'
3' UCAUGUAGUAGA**UAUGACA**U 5'

Site #2: 8mer 3365-3372
also conserved in Opossum
5'...UAAAUUCUGUAGUUUAUACUGUA...3'
3' UCAUGUAGUAGA**UAUGACA**U 5'

miR-144-3p targets in CHICKEN *dicer1* 3'UTR

Site #1: 7mer-A1 1562-1568
also conserved in Human, Chimp, Rhesus, Squirrel, Rabbit, Pig, Cow, Cat, Dog, Elephant, Opossum, Macaw, Lizard, X. tropicalis
5'...AAAUUUAAUUUUUGCACUGUAAC...3'
3' CUCAUGUAGUAGAUA**UGACAU**C 5'

Site #2: 8mer 4152-4159
also conserved in Opossum, Macaw, Lizard, X. tropicalis
5'...AAUGUAAUUCAUUCAUACUGUAA...3'
3' CUCAUGUAGUAGAUA**UGACAU**C 5'

Site #3: 7mer-m8 1232-1238
also conserved in Rhesus, Cat, Macaw, Lizard
5'...UCCACGUAAAUUUCUUACUGUAC...3'
3' CUCAUGUAGUAGAUA**UGACAU**C 5'

Site #4: 7mer-m8 1763-1769
also conserved in Cow, Cat, Dog, Brown Bat, Opossum, Macaw
5'...UAAAUUACAGAUAAAAUACUGUAU...3'
3' CUCAUGUAGUAGAUA**UGACAU**C 5'

Site #5: 7mer-m8 2794-2800
also conserved in Opossum, Macaw, Lizard
5'...UGUUUUUUUAAGUCAUACUGUAC...3'
3' CUCAUGUAGUAGAUA**UGACAU**C 5'

Site #6: 7mer-m8 3065-3071
also conserved in Macaw
5'...UGUCUGUGGCAUUUUUACUGUAU...3'
3' CUCAUGUAGUAGAUA**UGACAU**C 5'

Site #7 7mer-A1: 3759-3765
5'...GUAAUCUAAAUAUCAACUGUAAC...3'
3' CUCAUGUAGUAGAUA**UGACAU**C 5'

miR-144-3p targets in X. tropicalis *dicer1* 3'UTR

Site #1: 8mer 1782-1789
also conserved in Opossum, Macaw, Chicken, Lizard
5'...UCUCAAGGGACUUUCAUACUGUA...3'
3' AUCAUGUAGUAGAU**AUGACA**U 5'

Figure S3. Related to Figure 2.

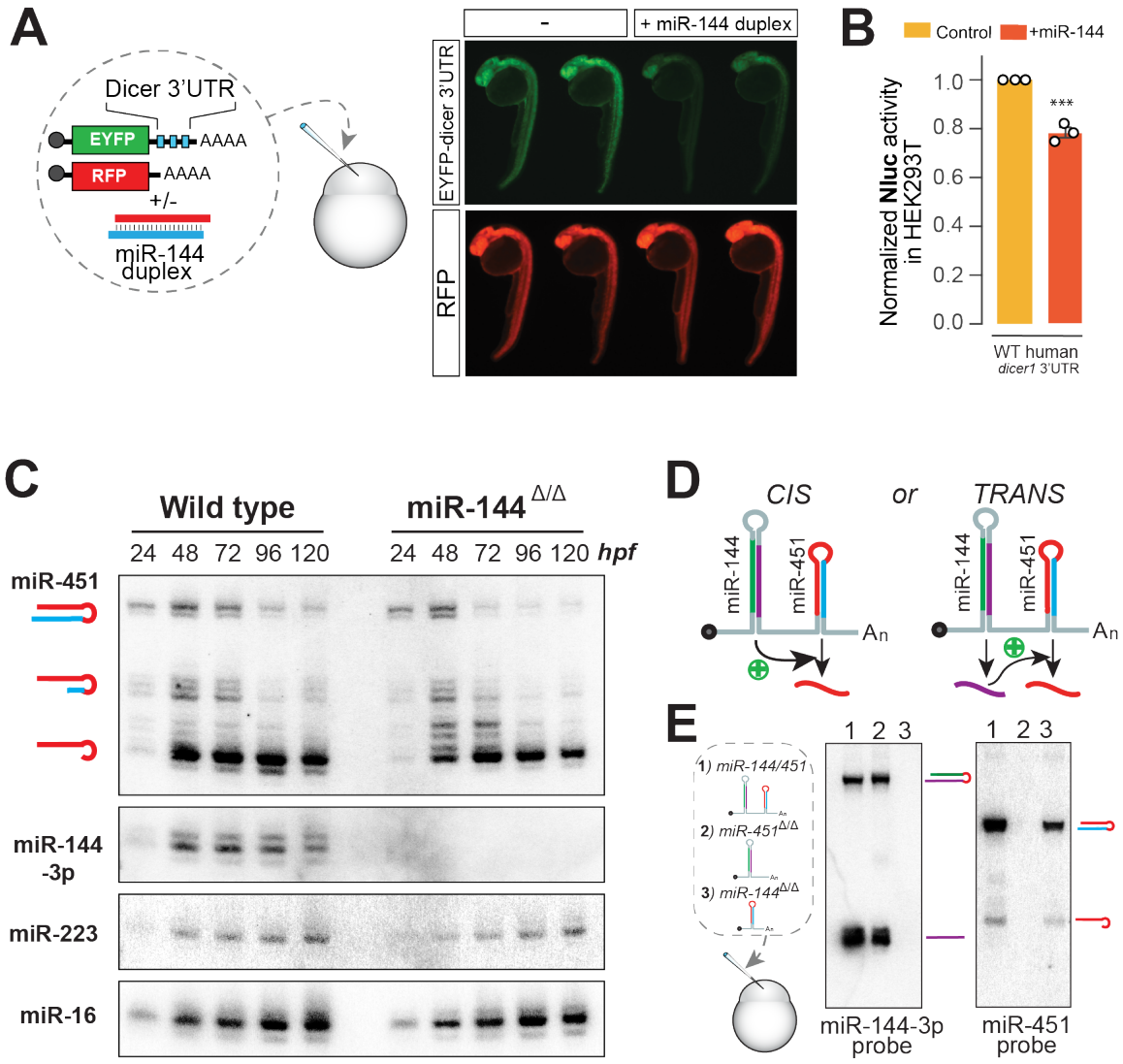

Figure S4. Related to Figure 3.

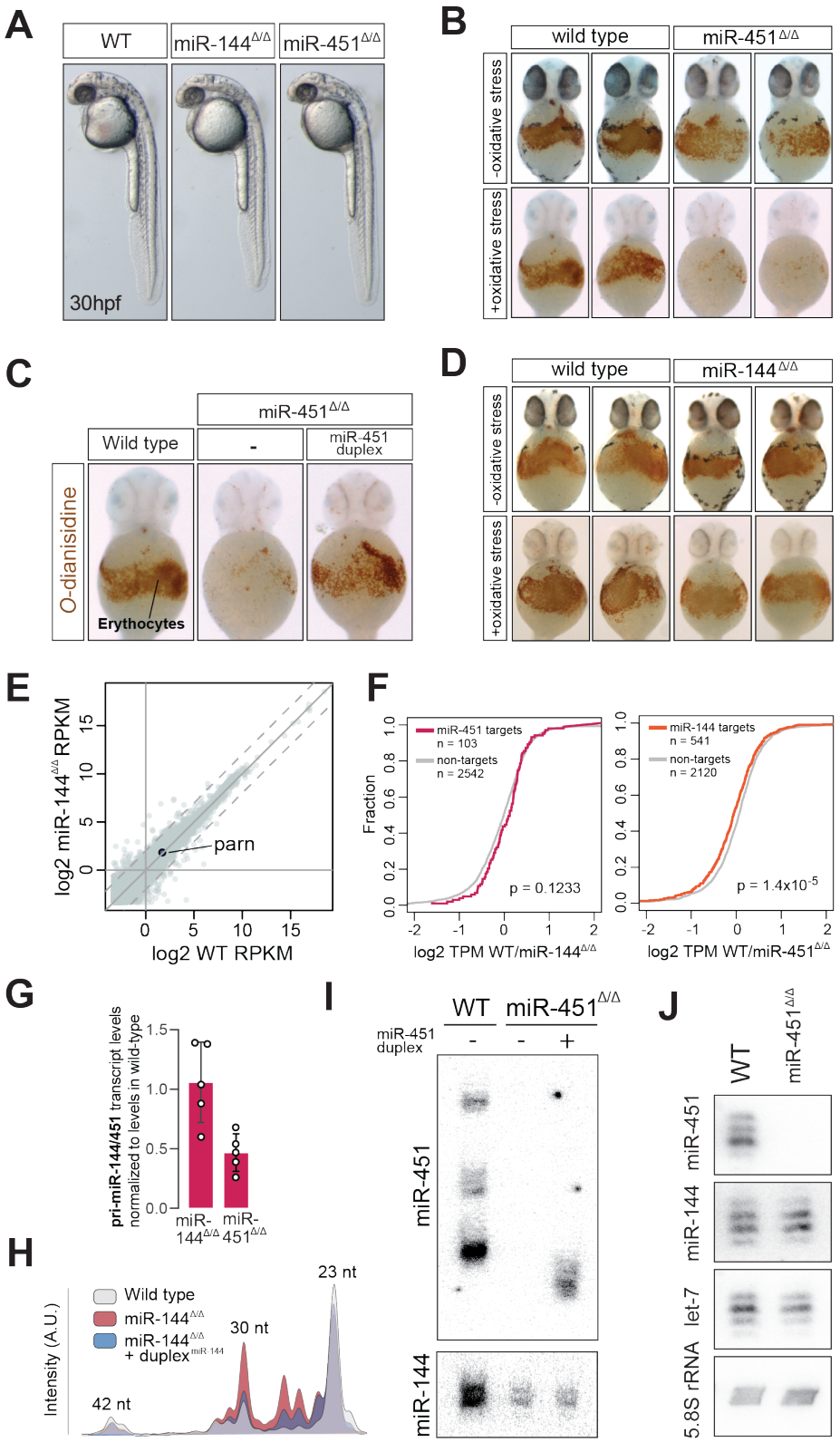

Figure S5. Related to Figure 4.

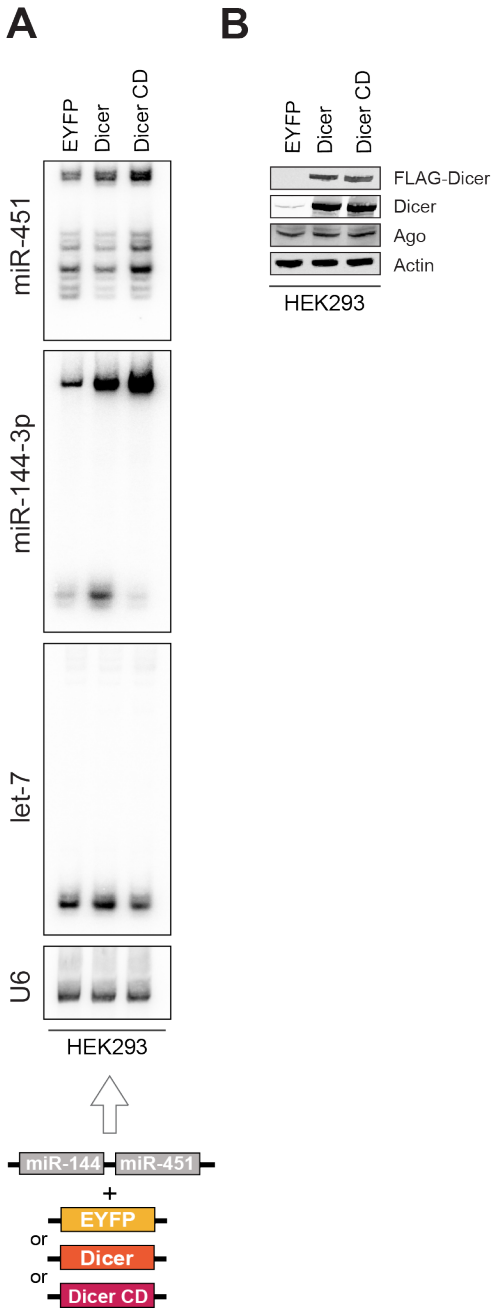

Figure S6. Related to Figure 5.

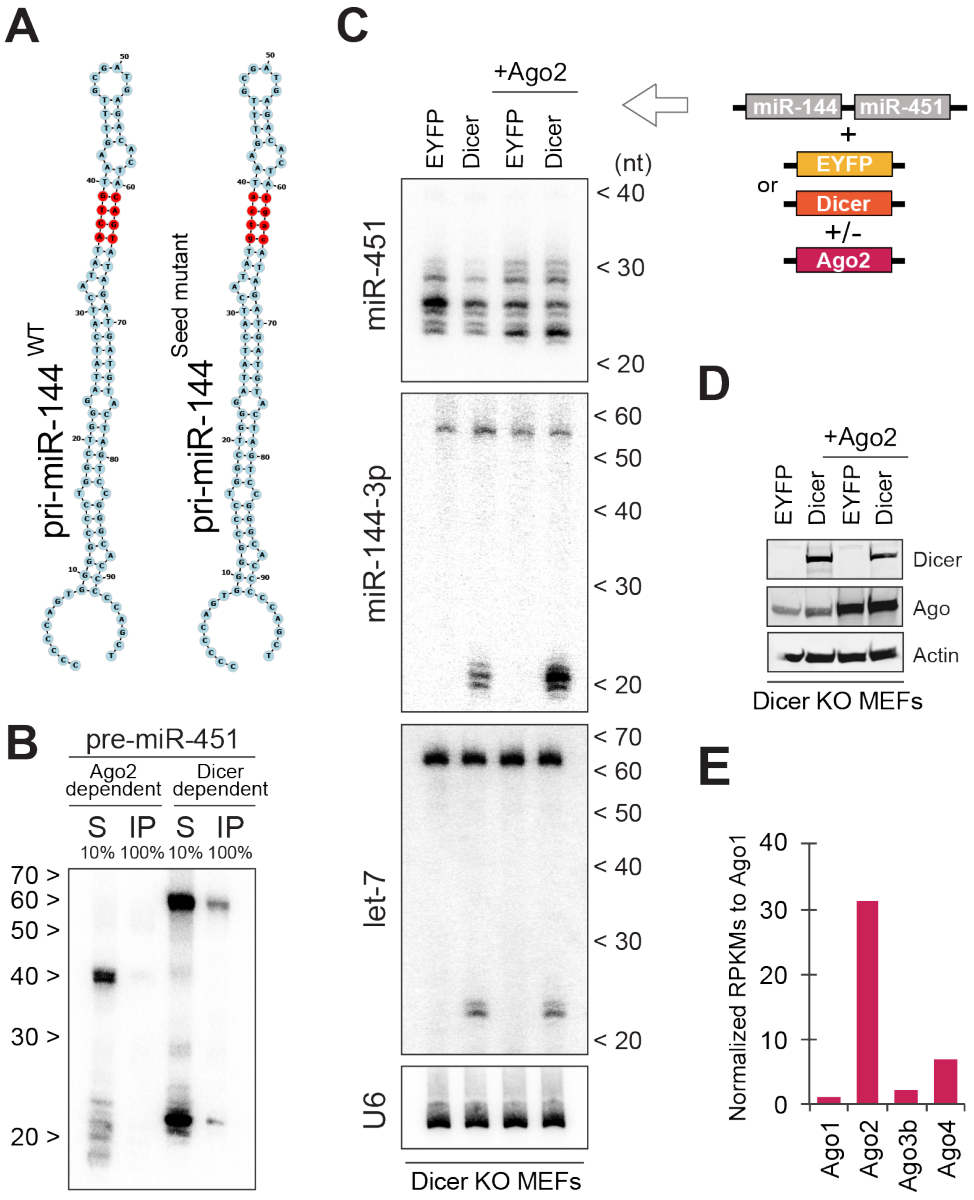

REFERENCES

AGARWAL, V., BELL, G. W., NAM, J. W. & BARTEL, D. P. 2015. Predicting effective microRNA target sites in mammalian mRNAs. *Elife,* 4.

BARTEL, D. P. 2018. Metazoan MicroRNAs. *Cell,* 173**,** 20-51.

BEREZIKOV, E., CHUNG, W. J., WILLIS, J., CUPPEN, E. & LAI, E. C. 2007. Mammalian mirtron genes. *Mol Cell,* 28**,** 328-36.

BRUCHOVA, H., MERKEROVA, M. & PRCHAL, J. T. 2008. Aberrant expression of microRNA in polycythemia vera. *Haematologica,* 93**,** 1009-16.

BRUCHOVA, H., YOON, D., AGARWAL, A. M., MENDELL, J. & PRCHAL, J. T. 2007. Regulated expression of microRNAs in normal and polycythemia vera erythropoiesis. *Exp Hematol,* 35**,** 1657-67.

CAZALLA, D., XIE, M. & STEITZ, J. A. 2011. A primate herpesvirus uses the integrator complex to generate viral microRNAs. *Mol Cell,* 43**,** 982-92.

CHELOUFI, S., DOS SANTOS, C. O., CHONG, M. M. & HANNON, G. J. A dicer-independent miRNA biogenesis pathway that requires Ago catalysis. *Nature,* 465**,** 584-9.

CIFUENTES, D., XUE, H., TAYLOR, D. W., PATNODE, H., MISHIMA, Y., CHELOUFI, S., MA, E., MANE, S., HANNON, G. J., LAWSON, N. D., WOLFE, S. A. & GIRALDEZ, A. J. 2010. A novel miRNA processing pathway independent of Dicer requires Argonaute2 catalytic activity. *Science,* 328**,** 1694-8.

DIEDERICHS, S. & HABER, D. A. 2007. Dual role for argonautes in microRNA processing and posttranscriptional regulation of microRNA expression. *Cell,* 131**,** 1097-108.

DORE, L. C., AMIGO, J. D., DOS SANTOS, C. O., ZHANG, Z., GAI, X., TOBIAS, J. W., YU, D., KLEIN, A. M., DORMAN, C., WU, W., HARDISON, R. C., PAW, B. H. & WEISS, M. J. 2008. A GATA-1-regulated microRNA locus essential for erythropoiesis. *Proc Natl Acad Sci U S A,* 105**,** 3333-8.

ENDER, C., KREK, A., FRIEDLANDER, M. R., BEITZINGER, M., WEINMANN, L., CHEN, W., PFEFFER, S., RAJEWSKY, N. & MEISTER, G. 2008. A human snoRNA with microRNA-like functions. *Mol Cell,* 32**,** 519-28.

GAUTIER, E. F., DUCAMP, S., LEDUC, M., SALNOT, V., GUILLONNEAU, F., DUSSIOT, M., HALE, J., GIARRATANA, M. C., RAIMBAULT, A., DOUAY, L., LACOMBE, C., MOHANDAS, N., VERDIER, F., ZERMATI, Y. & MAYEUX, P. 2016. Comprehensive Proteomic Analysis of Human Erythropoiesis. *Cell Rep,* 16**,** 1470-1484.

HAUSSECKER, D., HUANG, Y., LAU, A., PARAMESWARAN, P., FIRE, A. Z. & KAY, M. A. 2010. Human tRNA-derived small RNAs in the global regulation of RNA silencing. *RNA,* 16**,** 673-95.

INUKAI, S., PINCUS, Z., DE LENCASTRE, A. & SLACK, F. J. 2018. A microRNA feedback loop regulates global microRNA abundance during aging. *RNA,* 24**,** 159-172.

JEE, D., YANG, J. S., PARK, S. M., FARMER, D. T., WEN, J., CHOU, T., CHOW, A., MCMANUS, M. T., KHARAS, M. G. & LAI, E. C. 2018. Dual Strategies for Argonaute2-Mediated Biogenesis of Erythroid miRNAs Underlie Conserved Requirements for Slicing in Mammals. *Mol Cell,* 69**,** 265-278 e6.

LEE, D., PARK, D., PARK, J. H., KIM, J. H. & SHIN, C. 2019. Poly(A)-specific ribonuclease sculpts the 3' ends of microRNAs. *RNA,* 25**,** 388-405.

MARTELLO, G., ROSATO, A., FERRARI, F., MANFRIN, A., CORDENONSI, M., DUPONT, S., ENZO, E., GUZZARDO, V., RONDINA, M., SPRUCE, T., PARENTI,

A. R., DAIDONE, M. G., BICCIATO, S. & PICCOLO, S. 2010. A MicroRNA targeting dicer for metastasis control. *Cell,* 141**,** 1195-207.

NELSON, P. T., DE PLANELL-SAGUER, M., LAMPRINAKI, S., KIRIAKIDOU, M., ZHANG, P., O'DOHERTY, U. & MOURELATOS, Z. 2007. A novel monoclonal antibody against human Argonaute proteins reveals unexpected characteristics of miRNAs in human blood cells. *RNA,* 13**,** 1787-92.

OKAMURA, K., HAGEN, J. W., DUAN, H., TYLER, D. M. & LAI, E. C. 2007. The mirtron pathway generates microRNA-class regulatory RNAs in Drosophila. *Cell,* 130**,** 89-100.

PASE, L., LAYTON, J. E., KLOOSTERMAN, W. P., CARRADICE, D., WATERHOUSE, P. M. & LIESCHKE, G. J. 2009. miR-451 regulates zebrafish erythroid maturation in vivo via its target gata2. *Blood,* 113**,** 1794-804.

PATRICK, D. M., ZHANG, C. C., TAO, Y., YAO, H., QI, X., SCHWARTZ, R. J., JUN-SHEN HUANG, L. & OLSON, E. N. 2010. Defective erythroid differentiation in miR-451 mutant mice mediated by 14-3-3zeta. *Genes Dev,* 24**,** 1614-9.

RASMUSSEN, K. D., SIMMINI, S., ABREU-GOODGER, C., BARTONICEK, N., DI GIACOMO, M., BILBAO-CORTES, D., HOROS, R., VON LINDERN, M., ENRIGHT, A. J. & O'CARROLL, D. 2010. The miR-144/451 locus is required for erythroid homeostasis. *J Exp Med,* 207**,** 1351-8.

RISTORI, E., LOPEZ-RAMIREZ, M. A., NARAYANAN, A., HILL-TERAN, G., MORO, A., CALVO, C. F., THOMAS, J. L. & NICOLI, S. 2015. A Dicer-miR-107 Interaction Regulates Biogenesis of Specific miRNAs Crucial for Neurogenesis. *Dev Cell,* 32**,** 546-60.

RUBY, J. G., JAN, C. H. & BARTEL, D. P. 2007. Intronic microRNA precursors that bypass Drosha processing. *Nature,* 448**,** 83-6.

SHUKLA, S., BJERKE, G. A., MUHLRAD, D., YI, R. & PARKER, R. 2019. The RNase PARN Controls the Levels of Specific miRNAs that Contribute to p53 Regulation. *Mol Cell,* 73**,** 1204-1216 e4.

TREIBER, T., TREIBER, N. & MEISTER, G. 2019. Regulation of microRNA biogenesis and its crosstalk with other cellular pathways. *Nat Rev Mol Cell Biol,* 20**,** 5-20.

WIENHOLDS, E., KOUDIJS, M. J., VAN EEDEN, F. J., CUPPEN, E. & PLASTERK, R. H. 2003. The microRNA-producing enzyme Dicer1 is essential for zebrafish development. *Nat Genet,* 35**,** 217-8.

WONG, P., HATTANGADI, S. M., CHENG, A. W., FRAMPTON, G. M., YOUNG, R. A. & LODISH, H. F. 2011. Gene induction and repression during terminal erythropoiesis are mediated by distinct epigenetic changes. *Blood,* 118**,** e128-38.

XIE, M., LI, M., VILBORG, A., LEE, N., SHU, M. D., YARTSEVA, V., SESTAN, N. & STEITZ, J. A. 2013. Mammalian 5'-capped microRNA precursors that generate a single microRNA. *Cell,* 155**,** 1568-80.

YANG, J. S. & LAI, E. C. 2010. Dicer-independent, Ago2-mediated microRNA biogenesis in vertebrates. *Cell Cycle,* 9**,** 4455-60.

YANG, J. S., MAURIN, T., ROBINE, N., RASMUSSEN, K. D., JEFFREY, K. L., CHANDWANI, R., PAPAPETROU, E. P., SADELAIN, M., O'CARROLL, D. & LAI, E. C. 2010. Conserved vertebrate mir-451 provides a platform for Dicer-independent, Ago2-mediated microRNA biogenesis. *Proc Natl Acad Sci U S A,* 107**,** 15163-8.

YODA, M., CIFUENTES, D., IZUMI, N., SAKAGUCHI, Y., SUZUKI, T., GIRALDEZ, A. J. & TOMARI, Y. 2013. Poly(A)-specific ribonuclease mediates 3'-end trimming of Argonaute2-cleaved precursor microRNAs. *Cell Rep,* 5**,** 715-26.

YU, D., DOS SANTOS, C. O., ZHAO, G., JIANG, J., AMIGO, J. D., KHANDROS, E., DORE, L. C., YAO, Y., D'SOUZA, J., ZHANG, Z., GHAFFARI, S., CHOI, J.,

FRIEND, S., TONG, W., ORANGE, J. S., PAW, B. H. & WEISS, M. J. 2010. miR-451 protects against erythroid oxidant stress by repressing 14-3-3zeta. *Genes Dev,* 24**,** 1620-33.

ZHAN, M., MILLER, C. P., PAPAYANNOPOULOU, T., STAMATOYANNOPOULOS, G. & SONG, C. Z. 2007. MicroRNA expression dynamics during murine and human erythroid differentiation. *Exp Hematol,* 35**,** 1015-25.

ZHANG, L., FLYGARE, J., WONG, P., LIM, B. & LODISH, H. F. 2011. miR-191 regulates mouse erythroblast enucleation by down-regulating Riok3 and Mxi1. *Genes Dev,* 25**,** 119-24.

CellPress

KEY RESOURCES TABLE

REAGENT or RESOURCE	SOURCE	IDENTIFIER
Antibodies		
Anti-DICER	Abcam	ab227518
Anti-Flag M2	Sigma Aldrich	F1804
Anti-EIF2C2	Abnova	H00027161
Anti-Actin	Millipore	MAB1501R
IRDye 800CW Goat anti-mouse	Li-COR	925-32210
IRDye 680RD Goat anti-rabbit	Li-COR	926-68071
Bacterial and Virus Strains		
NEB 5-alpha Competent *E. Coli*	New England Biolabs	Cat#C2987H
Biological Samples		
DMEM	Corning	Cat#10013CV
Opti-MEM	Thermo Fisher Scientific	Cat#31985062
FBS	Thermo Fisher Scientific	Cat#10082147
Chemicals, Peptides, and Recombinant Proteins		
O-dianisidine	Sigma Aldrich	Cat#D9143-5G
N-Phenylthiourea	Sigma Aldrich	Cat#P7629
Hydrogen Peroxide Solution 30% W/W	Sigma Aldrich	Cat#HX0635-3
Trizol	Life Technologies	Cat#15596-018
ATP, [gamma-P32]	PerkinElmer	Cat#BLU502Z250UC
ATP, [alpha-P32]	PerkinElmer	Cat#BLU003H250UC
Anti-FLAG M2 Magnetic Beads	Sigma Aldrich	Cat#M8823
RNA Decade Markers	Thermo Fisher Scientific	Cat#AM7778
T4 PNK	New England Biolabs	Cat#M0201L
Klenow Fragment (exo-)	New England Biolabs	Cat#M0212S
SUPERase-In	Life Technologies	Cat#AM2696
NotI-HF	New England Biolabs	Cat#R3189L
SEQUEL™ NE REAGENT (PART A)	AmericanBio	Cat#AB13021-01000
SEQUEL™ NE DILUENT (PART B)	AmericanBio	Cat#AB13021201000
Zeta-Probe Membrane	Biorad	Cat#1620159
Giemsa stain, modified	Sigma Aldrich	Cat#GS500
May-Grünwald Stain	Sigma Aldrich	Cat#MG500
Critical Commercial Assays		
SuperScript III RT kit	Thermo Fisher Scientific	Cat#18080044
mMESSAGE mMACHINE SP6 transcription kit	Thermo Fisher Scientific	Cat#1340
mMESSAGE mMACHINE T7 transcription kit	Thermo Fisher Scientific	Cat#1345
Power SYBR green PCR Master Mix	Applied Biosystems	Cat#4367659
Nano-Glo Dual-Luciferease Reporter Assay	Promega	Cat#N1610
Monarch Plasmid Miniprep kit	New England Biolabs	Cat#T1010L
Monarch PCR&DNA Cleanup kit	New England Biolabs	Cat#T1030L
Monarch DNA gel extraction Kit	New England Biolabs	Cat#T1020L
PureLink HiPure Plasmid Midiprep Kit	Thermo Fisher Scientific	Cat#K210014

RNA Clean & Concentrator	ZymoReserach	Cat#R1017
ExpressHyb Hybridization Solution	Clontech	Cat#636831
Lipofectamine 3000 Transfection Reagent	Thermo Fisher Scientific	Cat#L3000008
Lipofectamine RNAiMAX Transfection Reagent	Thermo Fisher Scientific	Cat#13778150
Silencer Negative Control No. 1 siRNA	Thermo Fisher Scientific	Cat#AM4611
NuPAGE Transfer Buffer (20X)	Novex	NP0006-1
NuPAGE MOPS SDS Running Buffer (20X)	Novex	NP0001
Bradford Reagent	bioworld	L19040407
8% Tris-Glycine Gel	Novex	XP00080BOX
Nitrocellulose Membranes (0.45 μM)	Bio-Rad	1620115
TBE buffer 10X	Thermo Scientific	AM9865
SSC buffer 20X	Invitrogen	15557036
Deposited Data		
BioProject (NCBI)	PRJNA591815	https://dataview.ncbi.nlm.nih.gov/object/PRJNA591815?reviewer=8vjmpq6j9rp9je2kb8c9p4atga
Experimental Models: Cell Lines		
Human: HEK293T	ATCC	
MEF DICER KO	Dr. Eric Lai laboratory	
Experimental Models: Organisms/Strains		
Zebrafish	ZIRC	AB/TU
Zebrafish	ZIRC	TL/TLF
Zebrafish miR-451$^{\Delta/\Delta}$	This study	
Zebrafish miR-144$^{\Delta/\Delta}$	This study	
Zebrafish Ago2$^{\Delta/\Delta}$	Cifuentes et al. Science 2010	
Zebrafish Dicer$^{hu896/+}$	Wienholds et al. Nat. Genet 2003	
Oligonucleotides		
Synthetic pre-miR-451 hairpins (related to Fig. 1C and 1D)		
pre-miR-451 #1	AAACCGUUACCAUUACUGAGUUUAGUAAUGGUAAGGGUUCUG	
pre-miR-451 #2	AAACCGUUACCAUUACUGAGUUUAGaUAAUGGUAAGGGUUCUG	
pre-miR-451 #3	AAACCGUUACCAUUACUGAGUUAAAAAAAUAGUAAUGGUAAGGGUUCUG	
pre-miR-451 #4	AAACCGUUACCAUUACUGAGUUUCGGUCUCGUCGAAAGGAAACUCAGUAAUGGUAAGGGUucuc	
pre-miR-451 #5	AAACCGUUACCAUUACUGAGUUUCGGUCUCGUCGAAAGGAAACUCAcGUAAUGGUAAGGGUucuc	

pre-miR-451 #6	AAACCGUUACCAUUACUGAGUUgcaaguuuguAACUCAGUAAUGGUAAGGGUucuc	
pre-miR-451 #7	CUCAGUAAUGGUAGUGACUUUUAAGAACAUAUCCAAGCUAAAACCGUUACCAUUACUGAGUU	
Synthetic RNA oligos		
dre-miR-451_5p_RNA	AAACCGUUACCAUUACUGAGTT	
dre-miR-451_3p_RNA	CUCAGUAAUGGUAACGGUAUTT	
dre-miR-144_5p_RNA	GGAUAUCAUCGUAUACUGUAAGU	
dre-miR-144-3p_RNA	CUACAGUAUAGAUGAUGUACUA	
Northern blot probes		
miR-451	AACTCAGTAATGGTAACGGTTTGGCGGG	
miR-144-5p	ACTTACAGTATACGATGATATCCTGGCGGG	
miR-144-3p	TAGTACATCATCTATACTGTAGGCGGG	
miR-223-3p	GGGGTATTTGACAAACTGACAGCGGG	
miR-16	CACCAATATTTACGTGCTGCTAGGCGGG	
U6	ATTTGCGTGTCATCCTTGCGCAGGGCGGG	
Let-7	AACTATACAACCTACTACCTCAGGCGGG	
miR-21	TCAACATCAGTCTGATAAGCTAGGCGGG	
qPCR primers	*Forward*	*Reverse*
dre_GAPDH	GTGGAGTCTACTGGTGTCTTC	GTGCAGGAGGCATTGCTTACA
dre_actin	CATCCGTAAGGACCTGTATGCCAAC	CAGGGAGGCCAAGATGGAGC
dre_dicer1	CCTGCGCTCTGCACTTGTC	CGATCGGCGAAGCTCTGAATCC
dre_miR144/451 locus Set #1	GGACGACTGAAGACGCACAT	CCTGAGGAAGTTTTCTCCTGAA
dre_miR144/451 locus Set #2	CCTGTGGACAAACACAATCGC	TCCACTTGAGATGTTCTTCGTT
Custom 3' adaptor for small RNA cloning		
3' Adaptor-"CACA"	/5PHOS/N*NCACAAGATCGGAAGAGCACACGTCTGAACTCCAGTCAC/3ddC/	
3' Adaptor-"AGAG"	/5PHOS/N*NAGAGAGATCGGAAGAGCACACGTCTGAACTCCAGTCAC/3ddC/	

Custom RT oligo + 5' adaptor for small RNA cloning		
RT Cloning Primer	/5PHOS/NNNNAGATCGGAAGAGCGTCGTGTAGGGAAAGAGTGTAGATCTCGGTGGTCGC-(SPC18)-GGATCC-(SPC18)-GTGACTGGAGTTCAGACGTGTGCTC	
spike-ins for small RNA cloning		
1	/5PHOS/NNNNGATCTGAGCCACGANNNN	
2	/5PHOS/NNNNGACATCGCGTGGAGNNNN	
3	/5PHOS/NNNNGTCTATCTCGAACTNNNN	
4	/5PHOS/NNNNATCAATGACGAACGNNNN	
5	/5PHOS/NNNNCGGCTCTACGAATTNNNN	
CRISPR gRNAs		
gRNA miR-144/451 locus 1	TAATACGACTCACTATAGGGGGTCAACGAGCCTCTGAGTTTTAGAGCTAGAA	
gRNA miR-144/451 locus 2	TAATACGACTCACTATAGGTTCTGAAACTTTTGACAGGTTTTAGAGCTAGAA	
Genotyping oligos	*Forward*	*Reverse*
dre_miR-144/451 locus	GGCAATTAAACCGCTCTTCA	CGTTCTTTCTCTGTTTCCTTACTGGCC
Primers for Dicer 3' UTR amplification	*Forward*	*Reverse*
dre_Dicer1	CAAGTAGCTCGAGCCTCGCAAGTGTTAAGAAAAAGGTCAGGTC	CGTAATACGACTCACTATAGTTCGATCCATAAGGTGCAGAATGC
hsa_Dicer1	CAAGTAGCTCGAGCCTGGTGTTGGTCGAAGTTACAGGATTGC	CGTAATACGACTCACTATAGTTCGATCTGGATTCCAGTGATCCTCTGC
Primers for Dicer and Ago2 amplification	*Forward*	*Reverse*
dre_Dicer1	GCAGGATCCCATCGATTCGccaccATGgactacaaggacgacgacGACAAGGCTGGCCTACAGCTGG	GAGGCTCGAGAGGCCTTGtcagttgttttggacctgaggttggttgg
dre_Ago2	GCAGGATCCCATCGATTCGccaccATGgactacaaggacgacgacGACAAGTATCCCATTGGAGCAGCTGG	GAGGCTCGAGAGGCCTTGTCAGGCGAAGTACATGGTGCG

Gene Block for hs_miR-144/451 locus	CGAATTCAAGGCCTCGCCATGCTTCCTGTGCCCC CAGTGGGGCCCTGGCTGGGATATCATCATATACT GTAAGTTTGCGATGAGACACTACAGTATAGATGAT GTACTAGTCCGGGCACCCCCAGCTCTGGAGCCTG ACAAGGAGGACAGGAGAGATGCTGCAAGCCCAAG AAGCTCTCTGCTCAGCCTGTCACAACCTACTGACT GCCAGGGCACTTGGGAATGGCAAGGAAACCGTTA CCATTACTGAGTTTAGTAATGGTAATGGTTCTCTTG CTATACCCAGAAAACGTGCCAGGAAGAGGCCTCT AGAACTATA	
Gene Block for hs_miR-144(mutated_seed)/451 locus	CGAATTCAAGGCCTCGCCATGCTTCCTGTGCCCC CAGTGGGGCCCTGGCTGGGATATCATCATATgtcaT AAGTTTGCGATGAGACACTAtgacATAGATGATGTA CTAGTCCGGGCACCCCCAGCTCTGGAGCCTGACA AGGAGGACAGGAGAGATGCTGCAAGCCCAAGAAG CTCTCTGCTCAGCCTGTCACAACCTACTGACTGCC AGGGCACTTGGGAATGGCAAGGAAACCGTTACCA TTACTGAGTTTAGTAATGGTAATGGTTCTCTTGCTA TACCCAGAAAACGTGCCAGGAAGAGGCCTCTAGA ACTATA	
Gene Block for dre_miR-144//451(Dicer-dependent) locus	CAGGATCCCATCGATTCGGTGAGAAGACGTGTAA AGGTGACAGATGAAGGCAATTAAACCGCTCTTCAA CACTTCCTGCGGGACGACTGAAGACGCACATCTA AAGGTGAGTGTGGTGACTACGAACTACGGGACGG CAGATGCTCTTCCTCATCTGATGAAGAGTTCAATG TGATTCTGTGAAGAATTCAGGAGAAAACTTCCTCA GGAAGAAACTTCTTTAATTTAGACCATATAGATCAC TAATAAGGACGTTTCTGAAACTTTTGACAGTGGTC AAATGTGATTTTAGATGCATTTTTTCTGTTATGAAT GTCATTTAAATTGATTTTCTACAAAAAGACTTGATT GTTTTAATCTTGCTCTCTAGACAGGATATCATCGTA TACTGTAAGTTCATTATTGAGACACTACAGTATAGA TGATGTACTATCCAGGGGGTCAACGAGCCTCTGA CGGTTTCCTGTGGACAAACACAATCGCTGTGACAG AGAGAGGCGGCGAAACCGTTACCATTACTGAGTTT CGGTCTCGTCGAAAGGAAACTCAcGTAATGGTAAG GGTtctcCTGCCTTTTCTCAACAATCATCTGGATGTA AGAGAACGAAGAACATCTCAAGTGGAAGGCCTCT CGAGCCTCTAG	
Recombinant DNA		
pCS2-TagRFP	This study	N/A
pCS2-EYFP	This study	N/A
pCS2-EYFP-2XIPT-miR-451	This study	N/A
pCS2-EYFP-*Dre*-Dicer-3'-UTR	This study	N/A
pCS2-Firefly luciferase	This study	N/A
pCS2-NanoLuc-*Dre*-Dicer-3'UTR	This study	N/A
pCS2-NanoLuc-*Dre*-Dicer-3'UTR-144sites-mut	This study	N/A
pCS2-NanoLuc-*Hs*-Dicer-3'UTR	This study	N/A
pCS2- *Dre*-Dicer	This study	N/A
pCS2-*Dre*-Ago2	This study	N/A
pCS2-*Hs*-miR-144/451	This study	N/A
pCS2-*Hs*-miR-144(seed_mut)/451	This study	N/A

pCAGGS-FLAG-*Hs*Dicer	Phil Sharp Lab	Addgene (41584)
pCAGGS-FLAG-*Hs*Dicer (D1320A/D1709A)	Phil Sharp Lab	Addgene (41585)
pCS2-*Hs*-Dicer-3'UTR	This study	N/A
pCS2-*Mm*-Ago2	Cifuentes et al. Science 2010	
pCS2-*Dre*-miR-144/451	This study	N/A
pCS2-*Dre*-miR-144mut/451	This study	N/A
pCS2-*Dre*-miR-144/451mut	This study	N/A
pCS2-*Dre*-miR-144/451-Dicer-dependent	This study	N/A